AD-A150 230 1981 WC-130 AIRBORNE LIGHTNING CHARACTERIZATION PROGRAM 1/1
DATA REVIEW(U) AIR FORCE WRIGHT AERONAUTICAL LABS
WRIGHT-PATTERSON AFB OH B P KUHLMAN ET AL. AUG 84
UNCLASSIFIED AFWAL-TR-84-3024 F/G 4/1 NL

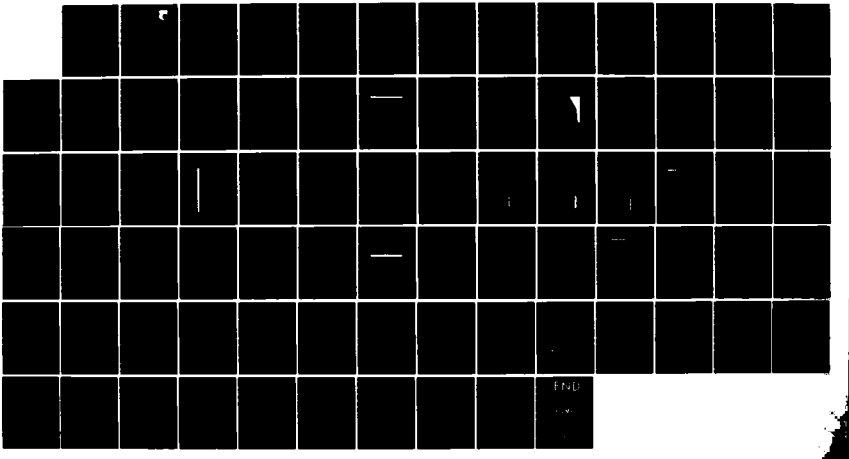

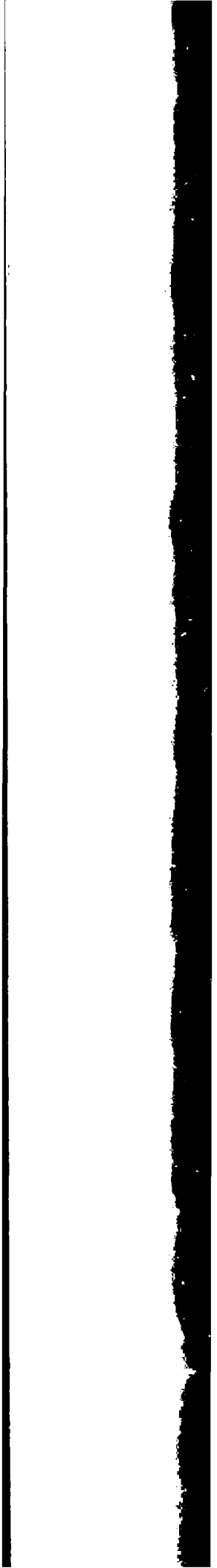

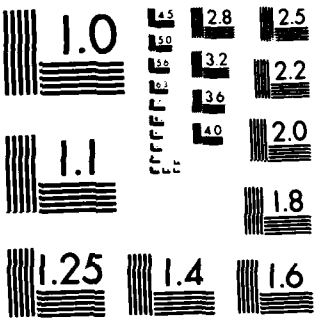

AFWAL-TR-84-3024

(12)

1981 WC-130 AIRBORNE LIGHTNING CHARACTERIZATION PROGRAM DATA REVIEW

B. P. Kuhlman
M. J. Reazer
P. L. Rustan

Flight Vehicle Protection Branch

August 1984

Interim Report for Period July 1981 - December 1983

Approved for Public Release; Distribution Unlimited.

FLIGHT DYNAMICS LABORATORY
AIR FORCE WRIGHT AERONAUTICAL LABORATORIES
AIR FORCE SYSTEMS COMMAND
WRIGHT-PATTERSON AIR FORCE BASE, OHIO 45433

NOTICE

When Government drawings, specifications, or other data are used for any purpose other than in connection with a definitely related Government procurement operation, the United States Government thereby incurs no responsibility nor any obligation whatsoever; and the fact that the government may have formulated, furnished, or in any way supplied the said drawings, specifications, or other data, is not to be regarded by implication or otherwise as in any manner licensing the holder or any other person or corporation, or conveying any rights or permission to manufacture use, or sell any patented invention that may in any way be related thereto.

This report has been reviewed by the Office of Public Affairs (ASD/PA) and is releasable to the National Technical Information Service (NTIS). At NTIS, it will be available to the general public, including foreign nations.

This technical report has been reviewed and is approved for publication.

BRIAN P. KUHLMAN, CAPT, USAF
Project Engineer

~~Pedro L. Rustan Jr, Chief~~
Atmospheric Electricity Hazards Group
Flight Vehicle Protection Branch
Vehicle E uipment Division

FOR THE COMMANDER

SOLOMON R. METRES
Director, Vehicle Equipment Division
Flight Dynamics Laboratory

"If your address has changed, if you wish to be removed from our mailing list, or if the addressee is no longer employed by your organization please notify AFWAL/FIESL, *W-PAFB, OH 45433 to help us maintain a current mailing list".*

Copies of this report should not be returned unless return is required by security considerations, contractual obligations, or notice on a specific document.

UNCLASSIFIED

SECURITY CLASSIFICATION OF THIS PAGE (When Data Entered)

REPORT DOCUMENTATION PAGE		READ INSTRUCTIONS BEFORE COMPLETING FORM
1. REPORT NUMBER AFWAL-TR-84-3024	2. GOVT ACCESSION NO. AD-A150 230	3. RECIPIENT'S CATALOG NUMBER
4. TITLE (and Subtitle) 1981 WC-130 AIRBORNE LIGHTNING CHARACTERIZATION PROGRAM DATA REVIEW		5. TYPE OF REPORT & PERIOD COVERED Interim Report July 1981 to December 1983 6. PERFORMING ORG. REPORT NUMBER
7. AUTHOR(s) Brian P. Kuhlman M. Jean Reazer* Pedro L. Rustan		8. CONTRACT OR GRANT NUMBER(s)
9. PERFORMING ORGANIZATION NAME AND ADDRESS Flight Dynamics Laboratory (AFWAL/FIESL) Air Force Wright Aeronautical Laboratories (AFSC) Wright Patterson Air Force Base, Ohio 45433		10. PROGRAM ELEMENT, PROJECT, TASK AREA & WORK UNIT NUMBERS 62201F 24020223
11. CONTROLLING OFFICE NAME AND ADDRESS Flight Dynamics Laboratory (AFWAL/FIESL) Air Force Wright Aeronautical Laboratories (AFSC) Wright Patterson Air Force Base, Ohio 45433		12. REPORT DATE August 1984 13. NUMBER OF PAGES 77
14. MONITORING AGENCY NAME & ADDRESS(if different from Controlling Office)		15. SECURITY CLASS. (of this report) Unclassified 15a. DECLASSIFICATION/DOWNGRADING SCHEDULE

16. DISTRIBUTION STATEMENT (of this Report)

Approved for public release; distribution unlimited.

17. DISTRIBUTION STATEMENT (of the abstract entered in Block 20, if different from Report)

18. SUPPLEMENTARY NOTES

*Technology/Scientific Services Inc.
Overlook Branch, P.O. Box 3065
Dayton, Ohio 45431

19. KEY WORDS (Continue on reverse side if necessary and identify by block number)

Airborne Lightning Characterization
Lightning Electromagnetic Fields
Lignting Risetimes
Lightning Waveforms

20 ABSTRACT (Continue on reverse side if necessary and identify by block number)

This report presents a review of airborne lightning data collected in late August 1981 by a WC-130 aircraft flying at 1500 to 18000 feet in the vicinity of thunderstorms over the Florida peninsula. Eleven electric and magnetic field sensors mounted on the aircraft provided outputs which were recorded both as continuous analog data with 2 megahertz bandwidth and as digital records of 164 microsecond windows with 20 megahertz bandwidth. Large amounts of data were collected for many parts of cloud-to-ground and intracloud lightning processes, including first and subsequent return strokes, stepped and dart-stepped leaders,

DD FORM 1 JAN 73 1473 EDITION OF 1 NOV 65 IS OBSOLETE

UNCLASSIFIED

SECURITY CLASSIFICATION OF THIS PAGE (When Data Entered)

20. Abstract (Continued)

preliminary breakdown pulses and intracloud pulses. Risetimes and field rates-of-change have been calculated and compared with ground-based measurements The data analyzed include 1034 lightning flashes from the analog record and 518 digital recordings, the latter including 347 return strokes, 68 events occurring ahead of the return stroke and 97 events from intracloud discharges. Submicrosecond risetimes were found in all the discharge phases analyzed and field rates-of-change for some intracloud processes approached rates-of-change for return strokes.

FOREWORD

This is the second Air Force technical report covering an ongoing research effort by the Atmospheric Electricity Hazards Group of the Flight Dynamics Laboratory (AFWAL/FIESL) to characterize the electromagnetic properties of lightning that may pose a threat to present and future generation aircraft. The first report titled "Airborne Lightning Characterization" (AFWAL-TR-83-3013) was published in January 1983. This research was performed under Subtask 2,"Lightning Characterization," Work Unit 24020223, "Atmospheric Electricity Hazard Assessment for Aircraft."

The data presented here were gathered during the summer of 1981 over the Florida peninsula using a WC-130 aircraft provided and operated by the Research Facility Center of the National Oceanic and Atmospheric Administration in Miami, Florida. The program was conducted in-house by Air Force personnel with valuable assistance from Technology/Scientific Services Incorporated.

The 1981 research flights were productive and resulted in the acquisition of large amounts of lightning data. Analysis of these data through various approaches has continued up to the present. This report contains the most complete description of the airborne WC-130 data that has been published to date. It is estimated that more than half of the data still remains to be examined in detail, and further results will be published in the near future.

The results presented were obtained through the dedicated efforts of several groups and individuals. Most of the data processing, preparation and preliminary analysis were completed by Technology/Scientific Services, Incorporated. Review of the large amounts of strip charts and waveform plots was accomplished through the patient efforts of Mr. Douglas Benner. Thanks are due to Dr. Frank Marks of the National Hurricane Research Laboratory in Miami for his assistance in the analysis of the airborne weather radar data.

TABLE OF CONTENTS

SECTION		PAGE
I	INTRODUCTION	1
II	INSTRUMENTATION	3
	1. Sensors	3
	2. Recording Equipment	5
	3. Other Instrumentation	7
III	DATA PROCESSING	8
	1. Objectives	8
	2. Techniques	9
IV	RESULTS	14
	1. Electric Field Record	14
	2. Digitally Recorded Data	22
V	DISCUSSION	62
VI	CONCLUSIONS	64
	REFERENCES	66

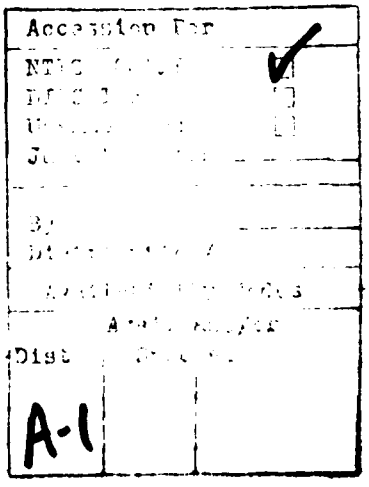

LIST OF ILLUSTRATIONS

FIGURE		PAGE
1	Sensor Installation on the WC-130 Aircraft	4
2	Airborne Instrumentation System Block Diagram	6
3	Time Code, Electric Field and DTR Trigger Pulse for a Multistroke Cloud-to-Ground Flash	10
4	Display from Airborne Weather Radar Data	13
5	Electric Fields for Some Cloud-to-Ground Flashes	18
6	Electric Fields for Cloud-to-Ground Flashes of Long Duration	19
7	Electric Fields for Three Intracloud Flashes	20
8	Electric Field Record of a Cloud-to-Ground Flash Preceded by an Intracloud Discharge	21
9	Distribution of the Number of DTR Return Stroke Records versus Return Stroke Number	24
10	DTR Magnetic Field Records Showing the First Return Stroke of a Cloud-to-Ground Flash	26
11	DTR Magnetic Field Records Showing the First Return Stroke of a Cloud-to-Ground Flash	27
12	DTR Magnetic Field Records Showing the First Return Stroke of a Cloud-to-Ground Flash	28
13	Magnetic Fields from Pulses after Initial Return Stroke Peak	29
14	DTR Magnetic Field Waveforms showing a Subsequent Return Stroke	31
15	DTR Magnetic Field Waveforms showing a Subsequent Return Stroke	32
16	DTR Magnetic Field Waveforms showing a Subsequent Return Stroke	33
17	DTR Magnetic Field Waveforms for a Subsequent Return Stroke Preceded by a Dart-Stepped Leader	34
18	DTR Magnetic Field Waveforms for a Subsequent Return Stroke Preceded by a Dart-Stepped Leader	35
19	DTR Magnetic Field Waveforms for a Subsequent Return Stroke Preceded by a Dart-Stepped Leader	36

LIST OF ILLUSTRATIONS (Concluded)

FIGURE		PAGE
20	Electric Field Record of a Multistroke Cloud-to-Ground Flash with Reversed Polarity	38
21	DTR Electromagnetic Field Records for the First Return Stroke Shown in Figure 20	39
22	Electric Field Record for a Cloud-to-Ground Flash with a DTR Trigger Pulse 250 μs Prior to the First Return Stroke	42
23	Analog Magnetic Field Record with DTR Trigger Pulse for the Flash Shown in Figure 22	42
24	DTR Magnetic Field Record Showing Leader Pulses from the Flash in Figure 23	43
25	Preliminary Breakdown Pulses	44
26	Analog Electric and Magnetic Field Record with a DTR Trigger Pulse at the Beginning of the Leader Process	46
27	DTR Magnetic Field Record Obtained at the Beginning of the Stepped Leader Process from the Flash in Figure 26	47
28	DTR Magnetic Field Records of Pulses Occurring Before the Stepped Leader Electric Field Change	48
29	Distribution of Time Intervals from DTR Trigger to First Return Stroke for DTR Records of Pre-Leader Pulses	48
30	DTR Magnetic Field Records Showing Pre-Leader Pulses	50
31	Expanded Plots of Pre-Leader Pulses from Figure 30	51
32	DTR Magnetic Field Records Showing Narrow Pulses from Intracloud Flashes	52
33	Expanded Plots of Intracloud Pulses from Figure 32	53
34	DTR Magnetic Field Record of a Bipolar Intracloud Pulse	53
35	DTR Magnetic Field Records Showing Intracloud Discharge Pulses	54
36	DTR Magnetic Field Records of Pulse Sequences during Intracloud Flashes	55
37	DTR Magnetic Field Records of Pulse Sequences during Cloud-to-Ground Flashes.	55

LIST OF TABLES

TABLE		PAGE
1	Analog Tape/Digital Record Summary	14
2	Lightning Flashing Rates from 25, 26 and 27 August Analog Data	16
3	Flashing Rates during the 26 August 1981 Storm	17
4	DTR Data Summary for 25, 26 and 27 August 1981	23
5	Lightning Electromagnetic Field Risetimes	58

SECTION I

INTRODUCTION

Over the thirteen year period from 1970 through 1982, 892 USAF aircraft lightning-related mishaps involving fifty-six aircraft types were reported. Interference in the form of an anomaly observed following a lightning strike was experienced in approximately one-fifth of the reported incidents; electrical damage was sustained in about one-twelfth of the reported incidents; and physical damage to structure was reported in roughly three-fourths of the incidents. Although these statistics reveal that all-metal aircraft are comparatively safe in a hazardous lightning environment, the introduction of non-metallic materials and structure and digitally-controlled flight-critical systems in new aircraft increase the concern as to their lightning vulnerability (References 1, 2, and 3).

In 1979, the Air Force Wright Aeronautical Laboratories (AFWAL) began a three year joint program with the National Oceanic and Atmospheric Administration (NOAA) with the purpose of acquiring a data base cn the electromagnetic parameters that characterize lightning, particularly at the high frequencies where bandwidth limited instrumentation had previously precluded measurements. To carry out the Lightning Characterization Program, a WC-130 Aircraft operated by NOAA was hardened against lightning, instrumented with wide bandwidth sensors and recorders and flown in the vicinity of active thunderstorms.

The program was evolutionary in that results from the first year (1979) were used to provide design criteria for improved instrumentation used in 1980 and 1981. Small amounts of data were obtained in 1979 and 1980 using systems described in an earlier report published by AFWAL titled "Airborne Lightning Characterization" (Reference 4).

During the third year of the program, a substantial amount of data was collected. A partial analysis of this data was completed and

reported in Reference 4. Correlated ground-based and airborne electromagnetic field measurements of several lightning strikes were analyzed and presented along with the results of a study of two direct strikes to the aircraft. To effectively carry out the processing and analysis of all the 1981 data, a general survey of the recordings was performed. The most complete set of data was obtained from various storms on three days near the end of August 1981. Airborne data obtained on these three days was examined to obtain preliminary lightning characteristics to direct further detailed study. This report describes how the data survey was conducted, outlines the type of data reviewed and summarizes the categories of data and characteristics observed.

SECTION II

INSTRUMENTATION

The aircraft instrumentation was designed with the ambitious intent to acquire a full spectrum of lightning information, from nearby and direct strike measurements to distant electromagnetic field measurements, from 0.1 hertz (Hz) up to 20 megahertz (MHz) bandwidth, from signal changes occurring in 40 nanoseconds (ns) to field changes lasting more than a second.

A full description of the sensors and instrumentation, calibration procedures and data retrieval techniques has been presented in Reference 4. A review of the relevant systems is given below.

1. SENSORS

Wide-bandwidth-derivative electric and magnetic field sensors manufactured by EG&G were installed on the upper and lower surfaces of the WC-130 aircraft as shown in Figures 1a and 1b, respectively. Two magnetic field loops (B-dot sensors) with their axes perpendicular to each other were mounted under a fiberglass pod on the centerline of the forward upper fuselage. Five similar magnetic field loops connected to less sensitive circuitry were also mounted on the aircraft, one on the upper and lower surface of each wing and one on the centerline of the aft upper fuselage. These acted as surface current sensors (J-dot) to measure skin currents on the aircraft. Three flush-plate dipole electric field sensors (D-dot sensors) were mounted on the aircraft, one on the centerline of the upper forward fuselage, one on the left wing tip, and one on the centerline of the lower aft fuselage below the aircraft tail. A hollow spherical dipole (Q-dot) electric field sensor was mounted on the centerline of the aft upper fuselage just forward of the tail. The signals were transmitted through fiber optics systems to recording instrumentation inside the aircraft. The sensors all had a frequency response greater than 38 MHz. Theory and design of the

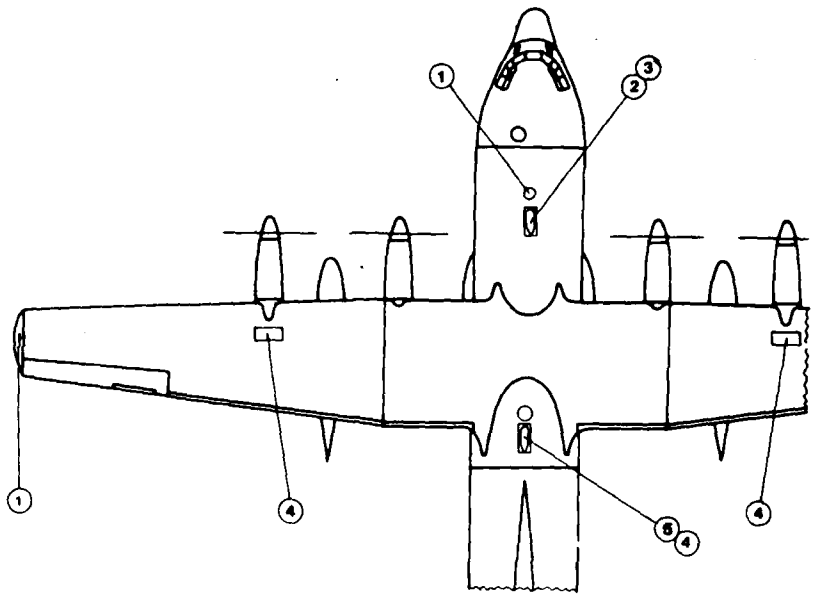

a. Top

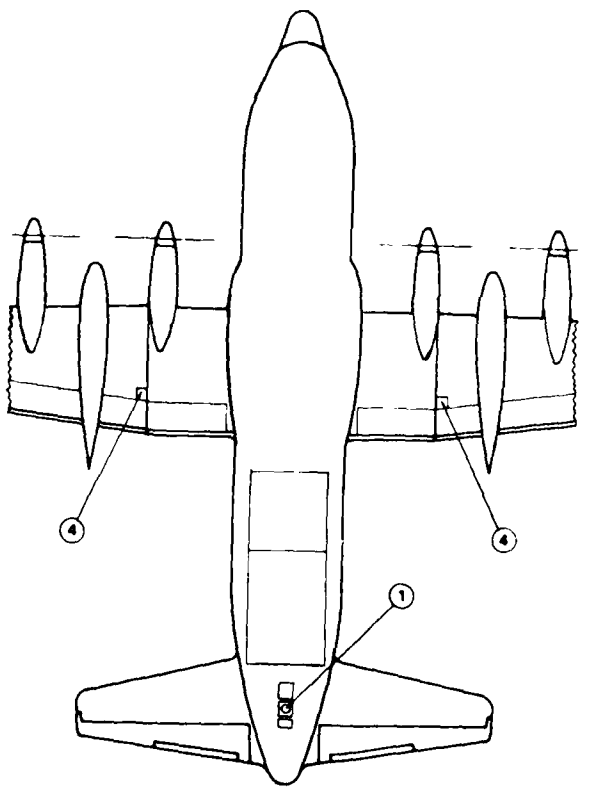

1 D Dot
2 B Dot (fuselage axis)
3 B Dot (wing axis)
4 J Dot
5 Q Dot

b. Bottom

Figure 1. Sensor Installation on the WC-130 Aircraft

sensors are discussed by Baum et al. in Reference 5. Detailed sensor and fiber optic system specifications are given in Reference 4.

2. RECORDING EQUIPMENT

A block diagram of the 1981 airborne instrumentation system is shown in Figure 2. Recording instrumentation consisted of a wideband digital transient recorder to record fast-changing transient signals, and a multichannel analog tape recorder to provide continuous recording over a longer time period. Signals from the fiber optic receivers were compressed with a semi-logarithmic function to reduce dynamic range prior to recording. Low pass filters with a -3 decibel cutoff frequency of 20 MHz were installed to minimize aliasing when the signals were digitized. Digitizing was accomplished with a 10-channel digital transient recorder (DTR) manufactured by MicroPro, Inc. When triggered, the recorder acquired 10 simultaneous records of 8192 data points sampled at 20 ns intervals for a time window of 164 microseconds (μs). Forty microseconds of pretrigger sampling were programmed into the recorder to record signals immediately preceding the trigger signal. The 10 channels of DTR data were encoded as a Manchester phase-modulated code and recorded on ten channels of the analog recorder. Approximately two 10 channel digital recordings could be captured and stored each second. Each time the DTR was triggered a pulse was recorded on a separate channel of the analog recorder marking the time that the digital data was acquired within the analog field record. After the DTR data was stored on tape, another pulse was sent out signifying that the digital recorder was again ready to acquire data. These two pulses are referred to as the trigger pulse and reset pulse.

A 28-channel Honeywell 101 recorder performed continuous multichannel analog recording of the electromagnetic field signals. Outputs from the D-dot sensors, the Q-dot sensor and the B-dot sensors were integrated electronically and recorded on direct channels of the analog tape recorder. Outputs from the J-dot sensors were recorded

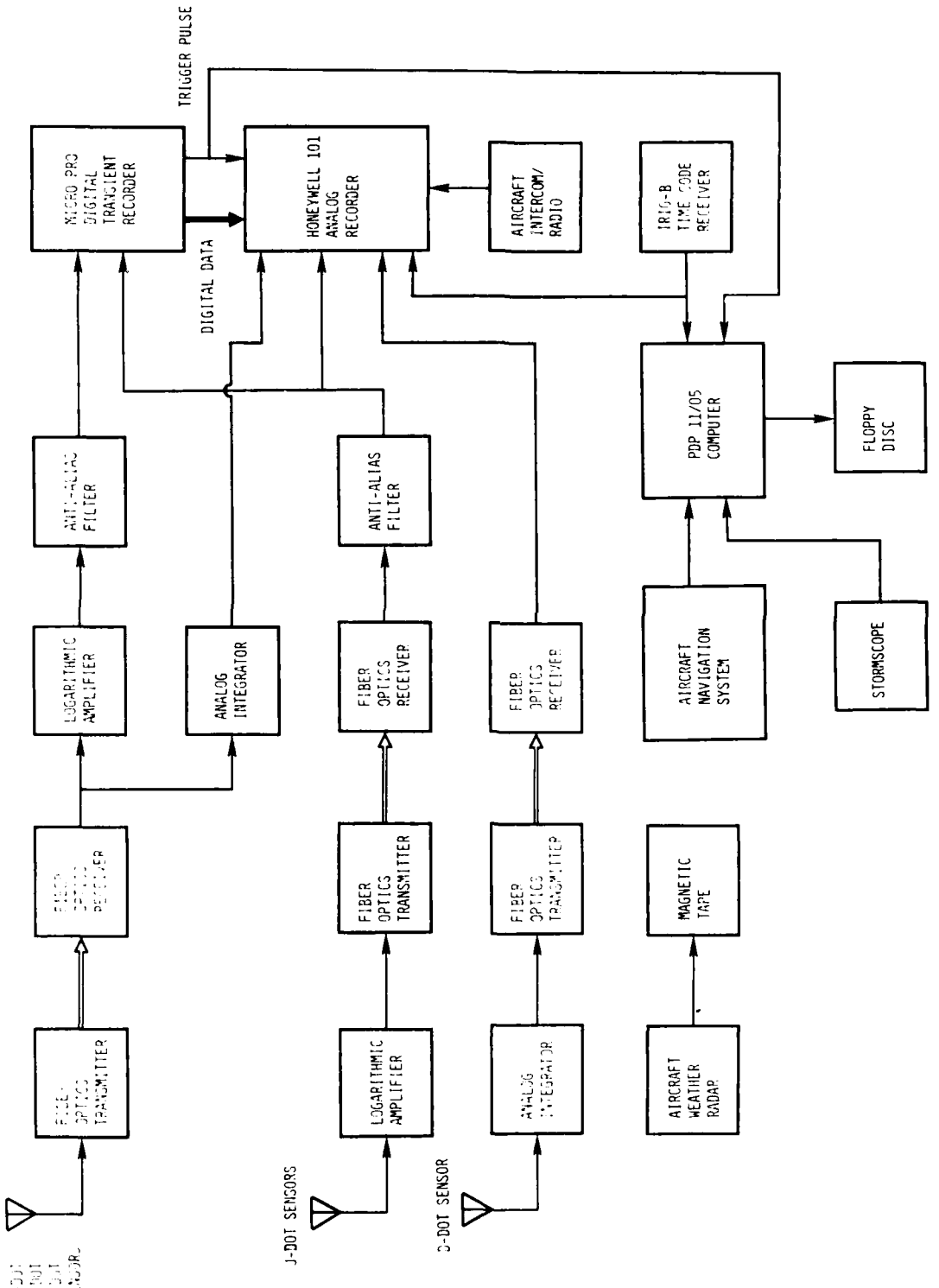

Figure 2. Airborne Instrumentation System Block Diagram

without integrating on other direct record channels. From 9 July to 21 August, the integrator electronics provided a bandwidth from 10 kilohertz (kHz) to 2 MHz. After 21 August, a modification in the electronics extended low frequency response to 3 kHz for all integrated sensor signals except the forward upper fuselage D-dot. This sensor was integrated with a long decay time and recorded on two FM channels of the recorder for an overall bandwidth from 0.1 Hz to 500 kHz. The Honeywell 101 was also used to record an IRIG-B time code signal, voice transmissions from the aircraft crew and the digital DTR data.

3. OTHER INSTRUMENTATION

Information on the aircraft heading, altitude and location was obtained from the aircraft's inertial navigation system and stored on floppy disk together with the DTR trigger time and file number, using a Digital Equipment Company (DEC) PDP-11 computer system.

A 3M/Ryan Stormscope Model WX-10 was mounted in the aircraft to estimate locations of electrical discharges and to direct the aircraft to electrically active areas.

Airborne weather radar with digital output was supplied by NOAA. Radar data were recorded on digital tape during flight to provide indications of precipitation contours in front of the aircraft for later correlation with the lightning data obtained. In the case of isolated storms, the radar data could be used to estimate the locations of lightning flashes.

In addition to the aircraft instrumentation, a network of ground-based VHF stations was set up to provide data to locate lightning VHF sources. An electric field station was also established to record ground based electric fields for comparison with airborne data. The ground-based systems, data and results are discussed in References 4, 6, and 7 and are not considered in this review.

SECTION III

DATA PROCESSING

1. OBJECTIVES

The objective of the data review was to discover all the categories of lightning data recorded by the DTR, to establish the context of the DTR data from the analog electric field record and to obtain preliminary characteristics of the different categories of DTR data to guide future research. Specific objectives were as follows:

a. To find out where in the overall lightning flash the digital recorder triggered and consequently what type of data is contained in the digital recordings.

b. To identify the time-domain characteristics of the digitally-recorded electromagnetic field waveforms which correspond to the different phases of lightning discharges.

c. To relate the digitally-recorded field characteristics to the overall electric field behavior and derive some understanding about the physical processes involved.

d. To determine the activity level of each thunderstorm by recording interval.

e. To determine general characteristics of lightning flashes observable in electric field records for comparison with previous studies and for interpretation of digital records.

f. To find estimates of lightning strike locations based on digitally-recorded radar echoes for correlation with electromagnetic field intensities.

g. To identify potential areas for further data reduction and analysis.

To accomplish these items, analog electric field signals from the tape recordings were replayed and plotted on a strip chart. The strip charts were examined and the characteristics observed were tabulated. In a similar manner, digitally-recorded DTR data were plotted, examined and grouped according to waveform characteristics. DTR data were then correlated with analog electric field data to categorize the data and to relate the waveforms to physical processes.

2. TECHNIQUES

To view the recorded electric field, measured on the forward upper fuselage sensor, the analog tapes were replayed at one-quarter of the recording speed and displayed on a Gould ES1000 electro-static strip chart recorder with a chart speed of 25 millimeters per second. By slowing the tapes down, a displayed upper bandwidth of four times the strip chart bandwidth was obtained. Since the ES-1000 has an upper bandwidth of 10 kHz, the strip charts displayed electric field data from 0.1 Hz to 40 kHz. Time resolution was limited to about 2 milliseconds (ms) due to the chart speed. IRIG-B time code and DTR trigger signals from the analog tape were also displayed on the strip chart so that the electromagnetic fields could be time-correlated with other data, and so the location of the digital recording could be placed in the overall event. The two-axis analog magnetic field recordings were also plotted on the chart to assist in evaluation of the electric field data. A section of strip chart displaying the various signals is shown in Figure 3. The record shows an electric field record typical of a multistroke cloud-to-ground flash, trigger and reset pulses indicating that the DTR captured the event at the beginning of the initial leader process, and time code indicating the time the event occurred. The wide vertical bars in the time code occur at 100 ms intervals as indicated in Figure 3.

The waveforms displayed on the strip charts were evaluated by comparing them with the patterns for cloud-to-ground and intracloud

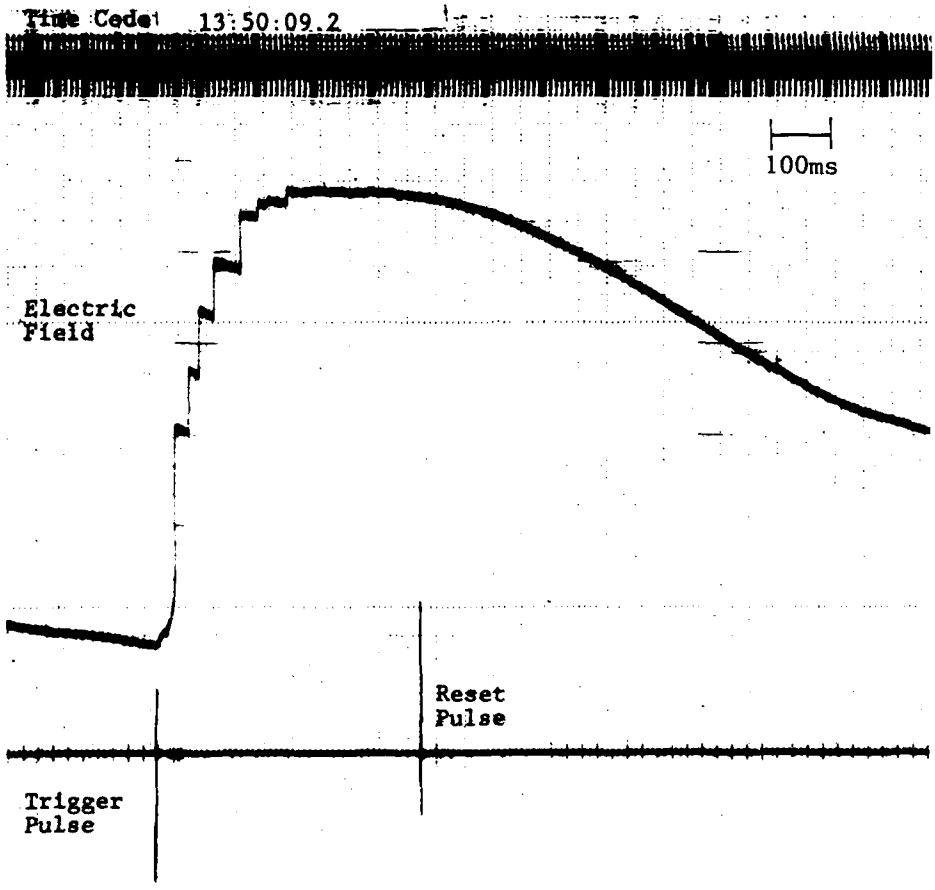

Figure 3. Time Code, Electric Field and DTR Trigger Pulse for Multistroke Cloud-to-Ground Flash

electric field changes observed in ground-based measurements. The strip chart records were examined to obtain the following data:

a. Percentages of intracloud and cloud-to-ground flashes

b. Percentage of cloud-to-ground flashes immediately preceded by intracloud discharges

c. Percentage of cloud-to-ground flashes with intervals of continuing current

d. Type of event triggering the DTR (intracloud or cloud-to-ground discharge)

e. Number of return strokes in each cloud-to-ground flash.

Analog electric field records are not scaled in this report since no inference is made from the electric field amplitudes but rather from the electric field waveshapes. Direct interpretation of aircraft electric fields is difficult due to the complexity of the experimental situation. The measured electric fields are generally not equal to the incident electric field but are a result of the incident field and field distortion introduced by the presence of the aircraft. This distortion can enhance the aircraft electric field over the value of the incident field producing a higher measured value (Reference 4). Often the aircraft was turning and changing orientation and position relative to the thunderstorm, changing the axis of sensitivity of the electric field sensor and decreasing or increasing measured electric field amplitudes. To further complicate the situation, electric field amplitudes and waveshapes produced by lightning discharges can be considerably different when measured at different locations above ground (Reference 8). Full analysis of all these factors is beyond the scope of this report.

After reviewing the electric field record, data files from the digital transient recorder were processed and reviewed. Processing involved retrieval, examination, storage, inverse-logging, scaling, integrating and plotting of the data.

Data files were retrieved from tape by replaying the data at 1/32 of recording speed and decoding the digital information through a MicroPro decoder unit. The decoder provided storage for ten data channels of 8192 samples with digital-to-analog reconstruction capability. This allowed display of each channel on an oscilloscope for viewing. The data files were then stored on floppy disk through the PDP-11 computer system for further analysis.

As previously mentioned, the time-rate-of-change data from the sensors had been compressed logarithmically to reduce dynamic range for recording. It was necessary, therefore, to expand the data, using the methods described in Reference 4. Integration and scaling of the data were performed with the PDP-11 using the trapezoidal approximation and the scale factors developed for the sensors. Waveforms were plotted on a Tektronix hard copy unit through a graphics terminal. After plotting, the waveshapes displayed were correlated with the trigger location in the electric field record so that the digital data could be categorized.

For some of the data, it was possible to estimate distance to the lightning using radar displays. Relative amplitudes of the initial peaks of the return stroke magnetic fields from the two B-dot sensors were used to estimate the azimuth of the lightning stroke in relation to the aircraft. The aircraft location and heading were then correlated with the return stroke azimuth data on charts showing airborne weather radar activity at the time the stroke occurred. In the cases where the storms were isolated, it was possible to determine approximate distance to the lightning activity from the radar echoes. One such weather radar plot is shown in Figure 4. The aircraft is located at the base of the arrow with the direction of the arrow indicating its heading. Dot density corresponds to contour level, with the darkest area indicating a level of 45 dBz or higher. An isolated thunderstorm is indicated off the nose of the aircraft at a distance of about 50 km.

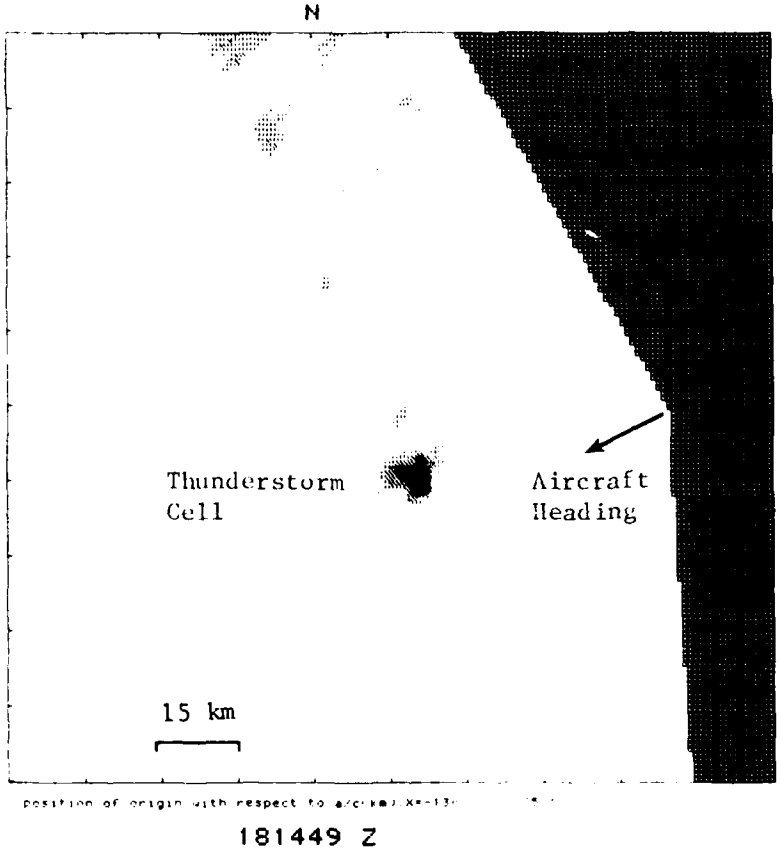

Figure 4. Display from Airborne Weather Radar Data

SECTION IV

RESULTS

1. ELECTRIC FIELD RECORD

Airborne electric field displays, produced from data recorded on the 25th, 26th and 27th of August 1981, were examined. Data acquired before this time period was not studied because the electric field system time constant was not long enough to permit full identification of the various phases of the discharge. A summary of all the recordings obtained in 1981 is given in Table 1. Around 14 hours of thunderstorm data are contained on the 58 analog tapes, including over 6000 10-channel DTR acquisitions.

TABLE 1

ANALOG TAPE/DIGITAL RECORD SUMMARY

Date (1981)	Number of Tapes (15 minutes each)	Number of Digital Records
9 July	3	59
15 July	4	531
16 July	7	963
17 July	5	610
22 July	2	129
23 July	5	549
31 July	8	750
7 Aug	3	214
21 Aug	5	328
25 Aug	7	524
26 Aug	7	1207
27 Aug	2	199
Total	58	6143

Review of the analog data from 25, 26 and 27 August revealed 1034 separate lightning flashes reproduced with enough resolution to study electric field characteristics. Table 2 shows the recording interval for each tape, the total number of discharges recorded, and an average flashing rate obtained by dividing the number of discharges by the recording interval. Combining all the events, except those from the first tape on the 26th of August where the radar shows no activity, gives an overall average flashing rate of 5.6 discharges per minute. Flashing rates range from 1.2 discharges per minute to 17.6 discharges per minute averaged over approximate 15 minute intervals. The flashing rates are within the range found by Piepgrass et al. (Reference 9) in Florida thunderstorms with a slightly higher overall average rate (5.6 discharges per minute compared to 3.3 discharges per minute). In some cases the flashing rates may include flashes from more than one thunderstorm cell.

The potential for rapid development of a thunderstorm and possibilities for sudden exposures of aircraft to lightning activity are illustrated by the data from Table 3 on 26 August where the flashing rate of 5.0 discharges/minute increases to 22.7 discharges/minute within six minutes as a storm builds up and the aircraft approaches it. The aircraft recorded data in the vicinity of this particular storm for approximately 45 minutes, experiencing flashing rates as shown in Table 3. At 17:08 the aircraft received a direct strike which disabled the radar and inertial navigation systems and no radar or aircraft position data are available after that time.

Examples of the electric field waveforms observed are shown in Figures 5 through 7. A variety of waveshapes appeared, from single stroke cloud-to-ground flashes as shown at the top of Figure 5, to long multistroke ground flashes as shown in Figure 6, to positive, negative and bipolar intracloud flashes, as shown in Figure 7. More than half of the discharges were intracloud (585 events or 57%) while 449 discharges (43%) went to ground. These percentages are the same as those found by Livingston and Krider for Florida thunderstorms (Reference 10). Fifteen percent of the cloud-to-ground flashes were immediately preceded by

TABLE 2

LIGHTNING FLASHING RATES FROM THE 25, 26 AND 27 AUGUST ANALOG DATA

Date	Tape Number	Time	Time Interval (minutes)	Number of Events	Events/ Minute	Radar Indications
25 Aug	1	13:47:29-13:55:16	7.75	70	9.0	No radar available
	2	14:14:8.9-14:28:28	14.3	51	3.6	Isolated activity then scattered activity
	3	15:19:47-15:34:20	14.5	41	2.8	Scattered activity
	4	15:45:13-16:00:40	15.5	68	4.4	Scattered activity
	5	16:04:08-16:19:01	14.9	100	6.7	Scattered activity
	6	16:27:10-16:41:38	14.5	44	3.0	Scattered activity
	7	16:48:13-17:01:43	13.5	16	1.2	Isolated activity
26 Aug	1	15:44:10-15:54:54	10.7	9	.84	No activity
	2	16:11:37-16:19:32	7.9	25	3.2	Scattered activity
	3	16:25:06-16:40:00	14.9	262	17.6	Scattered activity
	4	16:45:04-16:59:30	14.4	163	11.3	Scattered activity
	5	17:10:48-17:20:43	9.9	75	7.6	No radar available
	6	17:24:57-17:39:57	15.0	90	6.0	No radar available
	7	17:45:26-17:59:56	14.5	45	3.1	Scattered activity
27 Aug	1	17:30:17-17:40:19	10.0	13	1.3	Widely scattered activity
	2	17:45:38-17:56:04	10.4	25	2.4	Widely scattered activity

an intracloud discharge as shown in Figure 8. Approximately 37% of 338 cloud-to-ground flashes had intervals of continuing current, very close to 38% found by Livingston and Krider.

TABLE 3

FLASHING RATES DURING THE 26 AUGUST 1981 STORM

Tape	Time	Flashing Rate	Average Flashing Rate
238B	16:11:30-13:30	2.0	3.0
	13:30-15:30	2.5	
	15:30-17:30	2.5	
	17:30-19:30	5.0	
238C	16:25:00-28:00	22.7	17.3
	28:00-31:00	15.0	
	31:00-34:00	19.3	
	34:00-37:00	17.3	
	37:00-40:00	12.3	
238D	16:45:00-48:00	14.6	11.32
	48:00-51:00	7.3	
	51:00-54:00	10.6	
	54:00-57:00	11.3	
	57:00-59:30	12.8	
238E	17:08:00	*	
	17:11:00-14:00	8.7	7.6
	17:14:00-17:00	6.3	
	17:17:00-20:00	7.7	

* Direct strike - radar data ends

The number of return strokes per flash could not be accurately determined by counting abrupt steps in the electric field waveforms characteristic of return strokes. Some steps were less abrupt than others or much smaller than other steps in the same flash and therefore possibly due to discharge processes in the cloud rather than return strokes. More reliable identification of return strokes would require further data processing.

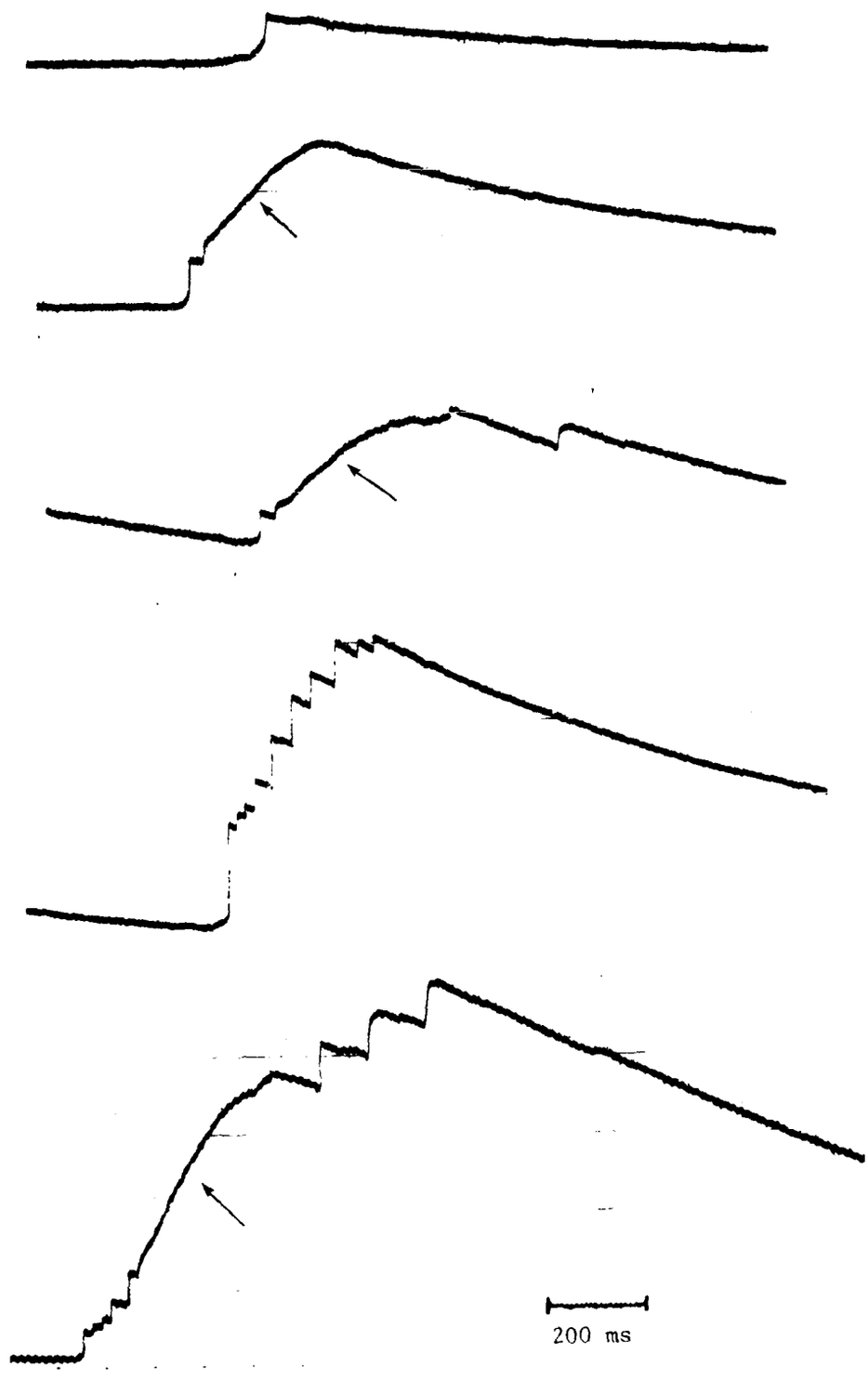

Figure 5. Electric Fields for Some Cloud-to-Ground Flashes the Arrows Point Out Intervals of Continuing Current

Figure 6. Electric Fields for Cloud-to-Ground Flashes of Long Duration

a. Negative Field Change

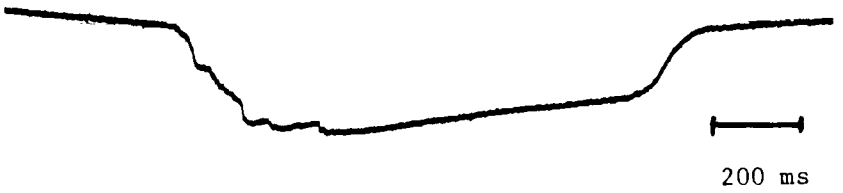

b. Positive Field Change

c. Bipolar Field Change

Figure 7. Electric Fields for Three Intracloud Flashes

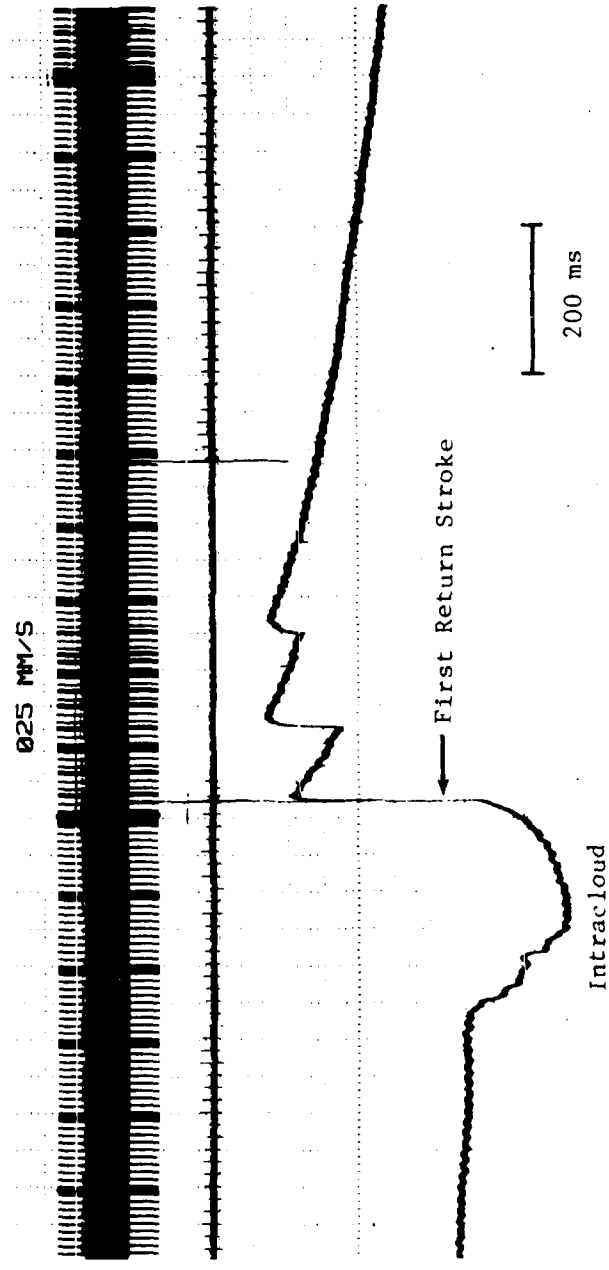

Figure 8. Electric Field Record of Cloud-to-Ground Flash
Preceded by an Intracloud Discharge

2. DIGITALLY RECORDED DATA

As shown in Table 1, 6143 DTR recordings were acquired during the 1981 summer research flights. The DTR was triggered and acquired data throughout the lightning flash for both intracloud and cloud-to-ground discharges. The majority of the data was acquired in the early part of the lightning flashes, usually on a first return stroke. Five hundred and eighty-four digital records from the 25, 26, and 27 August flights could be identified as a lightning discharge, either through the analog electric field record or the pattern of the digitally-recorded waveform. Signals from the two B-dot sensors and the Q-dot sensor for the 518 records were processed and plotted producing a variety of electromagnetic field waveshapes.

The digital records were divided into eight categories based on waveshape and time of DTR acquisition within the overall lightning flash. These categories were: a) pulses preceding stepped leader electric field changes, b) preliminary breakdown pulses, c) stepped leader pulses, d) first return strokes, e) subsequent return strokes preceded by a dart leader, f) subsequent return strokes preceded by a stepped leader, g) pulses after the first return stroke in cloud-to-ground flashes, and h) pulses recorded during intracloud discharges. Characteristics of the waveforms in each of these categories will be described followed by an analysis of the electromagnetic field risetimes and rates-of-change. The number of records obtained in each of the categories is given in Table 4.

a. Return Stroke Characteristics

The most hazardous lightning discharge phenomena is expected to be the return stroke of a cloud-to-ground flash. This is the first class of WC-130 DTR data that was studied. Correlated ground and airborne electromagnetic fields from 1981 data for several cloud-to-ground flashes were analyzed by Rustan et al. in Reference 4. A study of airborne electromagnetic field risetimes is presented in Reference 4

for 1979, 1980 and 1981 WC-130 data and in Reference 11 for several hundred return strokes recorded in 1981. No further return stroke risetime data are included in this report but general return stroke waveform characteristics are described and return stroke field risetimes and rates-of-change from Reference 11 are compared with other categories of DTR recorded data.

TABLE 4

DTR DATA SUMMARY FOR 25, 26 AND 27 AUGUST 1981

Category	Number of Records Acquired	%
a) Pulses Preceding Stepped Leader Electric Field Changes	48	9
b) Preliminary Breakdown Pulses	12	2
c) Stepped Leader Pulses	8	2
d) First Return Strokes	251	48
e) Subsequent Return Strokes Preceded by a Dart Leader	69	13
f) Subsequent Return Strokes Preceded by a Stepped Leader	27	5
g) Pulses After the First Return Stroke in Cloud-to-Ground Flashes	6	19
h) Pulses Recorded During Intracloud Flashes	97	19
Total	518	100

Three hundred and forty-seven return stroke waveforms were acquired by the DTR during the 25, 26, and 27 August flights, making up 67% of the identifiable DTR data from these days. Two hundred and forty-one of these return strokes were identified in the analog electric field record. The remaining return strokes recorded by the DTR did not produce sufficient amplitude in the analog electric field record to

clearly identify return stroke field changes due to the distance of the flashes. A histogram showing the number of DTR records acquired for each return stroke number for the 241 identified events is given in Figure 9. The return stroke number is obtained by counting return strokes from the first return stroke to the return stroke triggering the DTR as indicated by the DTR trigger pulse for each flash. Often the second return stroke in the flash produced a higher field transient at the aircraft than the first return stroke and activated the first DTR acquisition for that flash as can be seen from Figure 9.

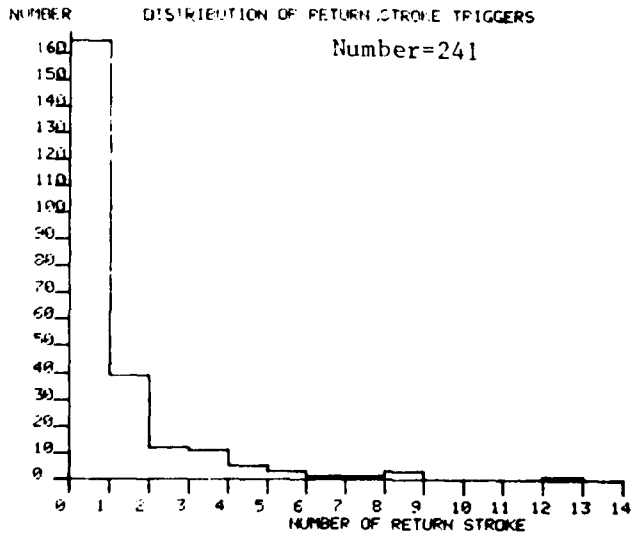

Figure 9. Distribution of the Number of DTR Return Stroke Records Versus Return Stroke Number

The structure of lightning return stroke electromagnetic fields on a microsecond time scale has been described by Weidman and Krider (Reference 12), Uman et al. (References 13 and 14), and Lin et al. (Reference 15). Most of the information presented in the literature on the structure of the electromagnetic fields of lightning appears to be from measurements of electric fields. Recently some researchers have

made wide-bandwidth measurements of lightning electromagnetic field rates-of-change. These measurements are generally over short time intervals or from very close flashes. Weidman and Krider made measurements of electric field rates-of-change from lightning return strokes and cloud discharges over a recording interval of 500 ns (Reference 16). Baum et al. have made measurements of magnetic and electric field rates-of-change from nearby lightning leader pulses and return strokes over a 20 μs recording interval (Reference 17). Data from the WC-130 measurements consisted of simultaneous electric and magnetic field rates-of-change on the surface of the aircraft from nearby and distant lightning over a 164 μs recording interval. Electromagnetic field derivatives and electromagnetic fields both were found to produce distinctive patterns in the waveforms for return strokes. Airborne measurements of three first return strokes are shown in Figures 10, 11 and 12. The first plot in each figure (a) shows the overall analog electric field record, DTR trigger pulse and time code, the second trace (b) shows the derivative magnetic field data recorded by the DTR at the time of the DTR trigger, and the third plot (c) shows the integration of the derivative field data from (b). The magnetic field time rate-of-change, plotted in each figure, shows high frequency variations throughout the waveform punctuated by sharp impulses at the time of the stepped leader pulses and the initiation of the return stroke. The amplitude of the high frequency variations increases slightly after the beginning of the return stroke and then decays slowly over the next 100 μs. When integrated, the data produces field waveshapes similar to electric fields measured on the ground with a series of leader pulses leading up to the first return stroke, a slow ramp initiating the return stroke followed by a fast transition to peak, and a series of large subsidiary peaks 10 to 30 μs apart after the start of the return stroke. Superimposed on the field after the start of the return stroke are a number of small, fast pulses which are the source of the high frequency variations in the derivative field record. These pulses were noted by Weidman and Krider in Reference 12.

From a random sample of twelve waveforms, the ratio of peak magnetic field derivative associated with the small pulses to the peak

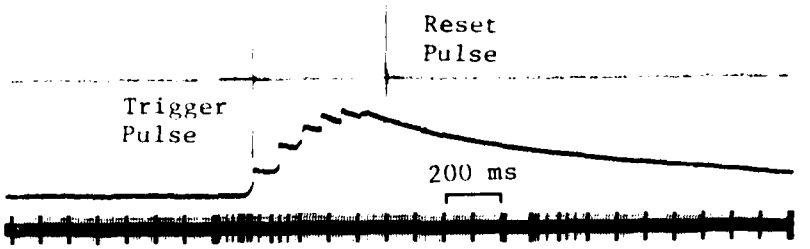

a. Analog Electric Field Record

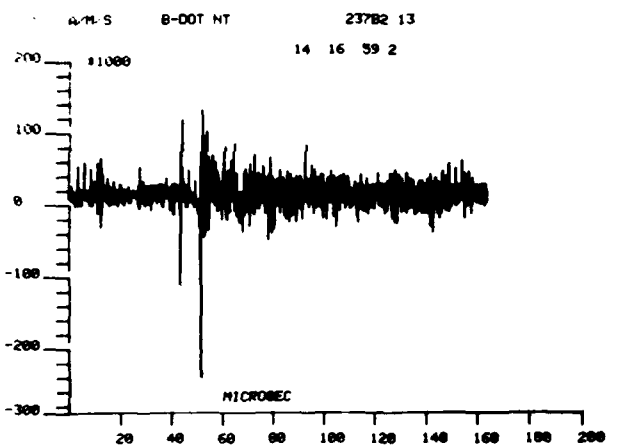

b. DTR Magnetic Field Derivative Record

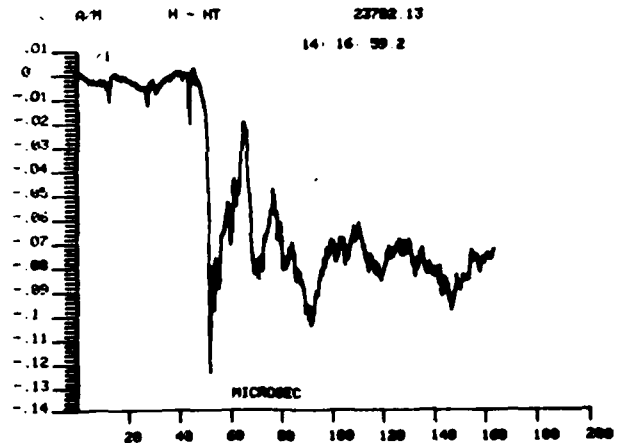

c. Magnetic Field (Integration of b.)

Figure 10. DTR Magnetic Field Records Showing the First Return Stroke of a Cloud-to-Ground Flash. The Top Plot (a) Shows the Overall Analog Electric Field Record with a Trigger Pulse Marking the time of DTR Data Acquisition

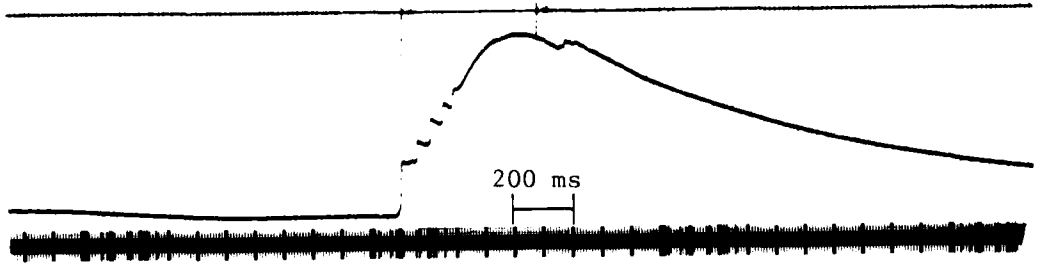

a. Analog Electric Field Record

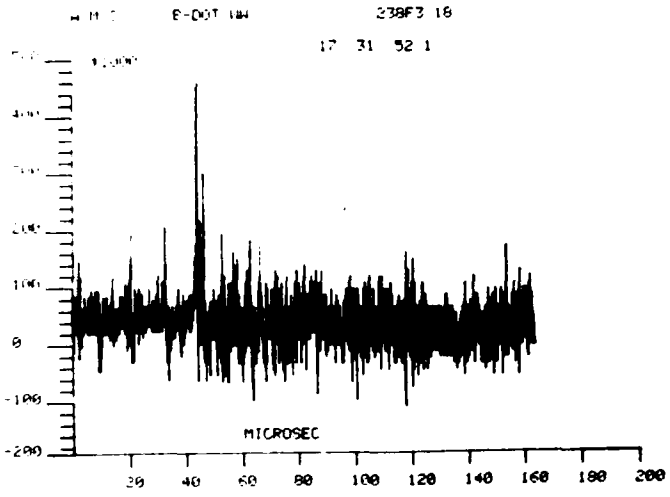

b. DTR Magnetic Field Derivative Record

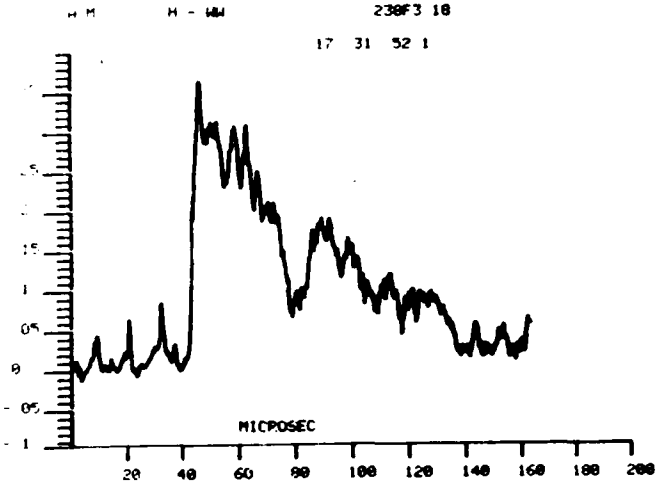

c. Magnetic Field (Integration of b.)

Figure 11. DTR Magnetic Field Records Showing the First Return Stroke of a Cloud-to-Ground Flash

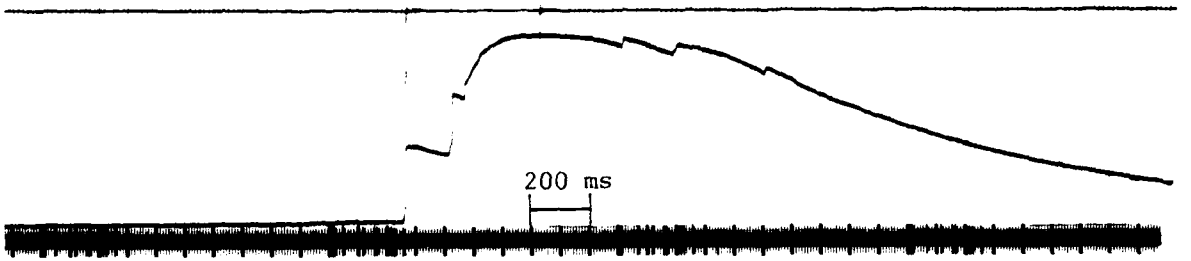

a. Analog Electric Field Record

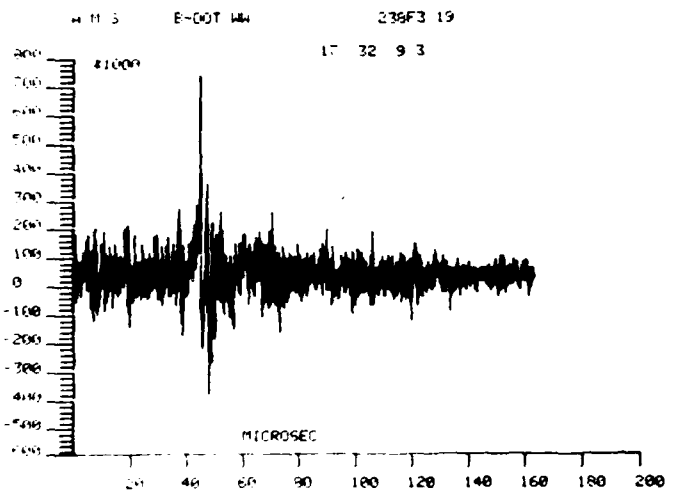

b. DTR Magnetic Field Derivative Record

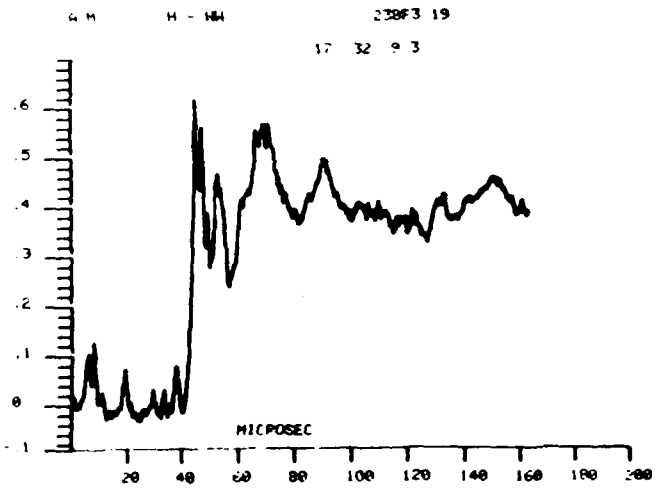

c. Magnetic Field (Integration of b.)

Figure 12. DTR Magnetic Field Records Showing the First Return Stroke of a Cloud-to-Ground Flash

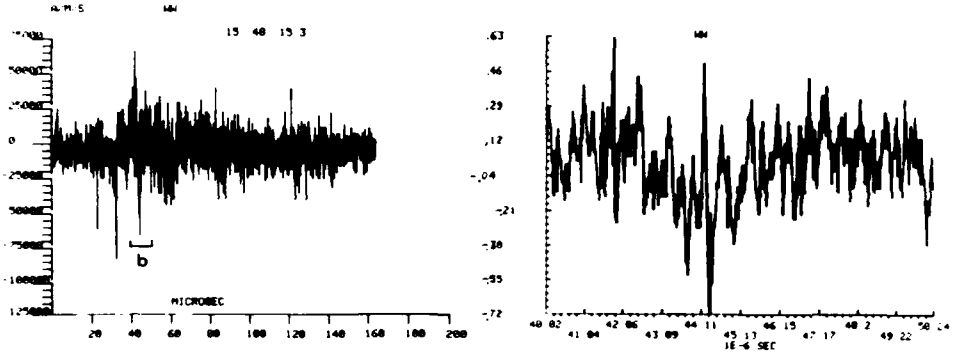

a. Overall Magnetic Field Derivative

b. Normalized Magnetic Field Derivative - Expanded

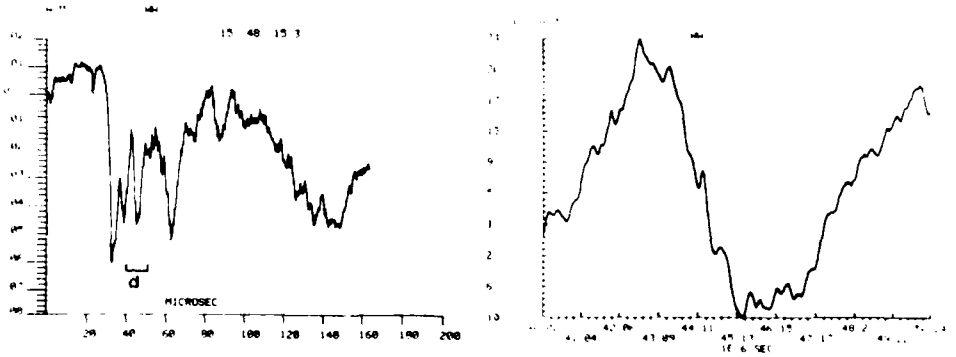

c. Overall Magnetic Field

d. Expanded Magnetic Field Corresponding to b.

Figure 13. Magnetic Fields from Pulses After Initial Return Stroke Peak

return stroke magnetic field derivative ranged from 0.2 to 0.9 with an average ratio of 0.4. For comparison, the ratio of peak magnetic field derivatives of leader pulses to the peak return stroke magnetic field derivative for the same twelve waveforms ranged from 0.2 to 0.7 with an average ratio of 0.3. One example is shown in Figure 13. The magnetic field rate-of-change is expanded in Figure 13b and normalized by dividing by the peak return stroke rate-of-change. The corresponding magnetic field waveshape is obtained by integrating and is shown in Figure 13d. The small pulses producing the large magnetic field rates-of-change can be seen in the magnetic field waveform but are overshadowed by the larger slower field change from the second subsidiary peak of the return stroke. Levine and Krider have made measurements of RF radiation correlated with wideband electric field measurements for first return strokes (Reference 18). They show HF and VHF radiation rising to a peak about 10 to 30 μs after the start of the return stroke. The radiation probably results from the discharges producing the small pulses in the field record although the magnetic field derivative peaks tend to decrease in the 100 μs following return stroke initiation while the RF radiation appears to increase.

Subsequent return strokes are differentiated from first return strokes in both the derivative and integrated field record by the absence of high frequency structure after initiation of the return stroke. Also, the high frequency variations during the leader just ahead of the return stroke (up to 40 μs ahead) have a smaller amplitude compared to the return stroke peak than those ahead of first strokes. After integration, the field record is relatively smooth following initiation of the return stroke and has a similar appearance to the ground data of Weidman and Krider. Examples of subsequent return stroke waveforms are shown in Figures 14 through 16.

Some subsequent return strokes were preceded by leader pulses as shown in Figures 17 through 19. These records are classified as subsequent return strokes because they occur after another return stroke in the same flash and because they lack high frequency variations in the derivative and integrated field records after the

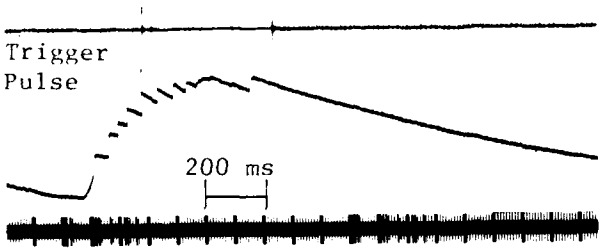

a. Analog Electric Field Record

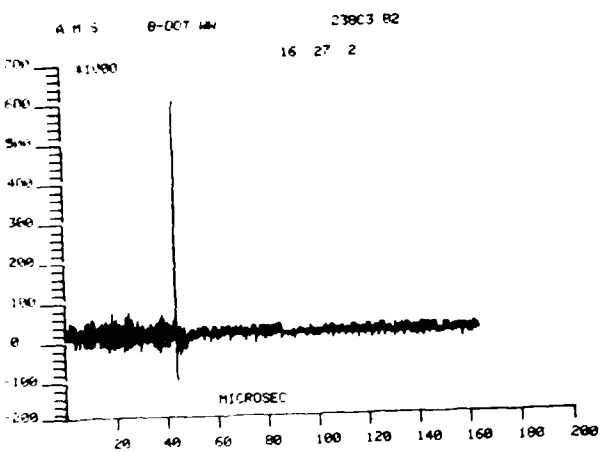

b. DTR Magnetic Field Derivative Record

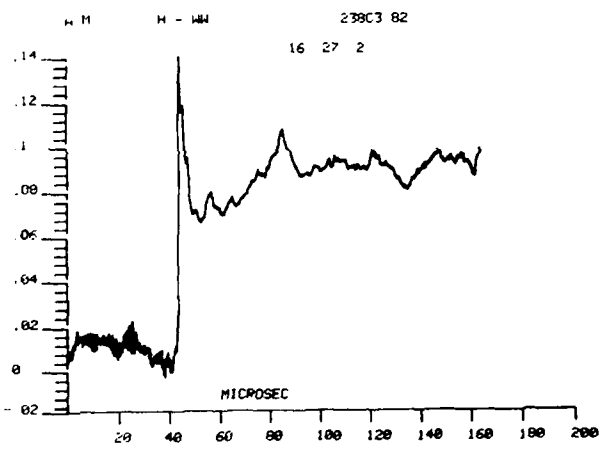

c. Magnetic Field (Integration of b.)

Figure 14. DTR Magnetic Field Waveforms Showing a Subsequent Return Stroke. The Top Plot (a) Shows the Overall Analog Electric Field Record With a Trigger Pulse Marking DTR Acquisition on the Fifth Return Stroke

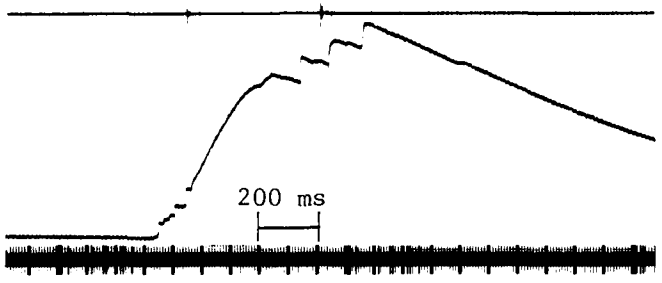

a. Analog Electric Field Record

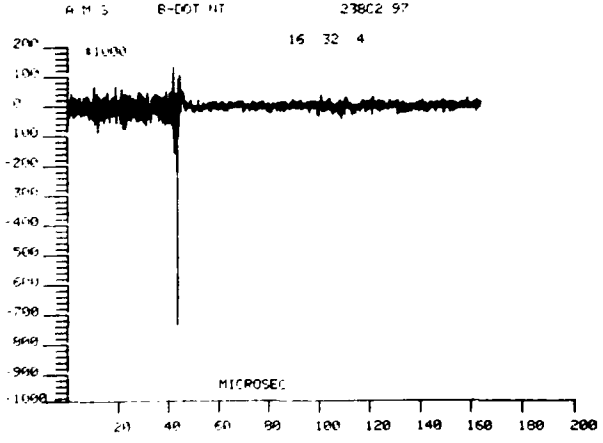

b. DTR Magnetic Field Derivative Record

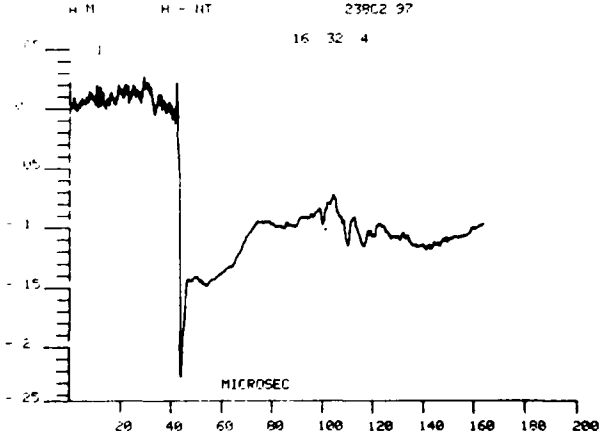

c. Magnetic Field (Integration of b.)

Figure 15. DTR Magnetic Field Waveforms Showing a Subsequent Return Stroke

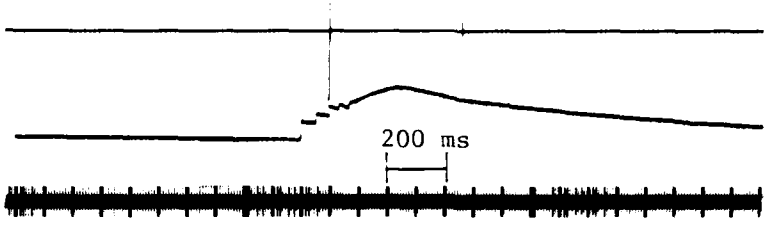

a. Analog Electric Field Record

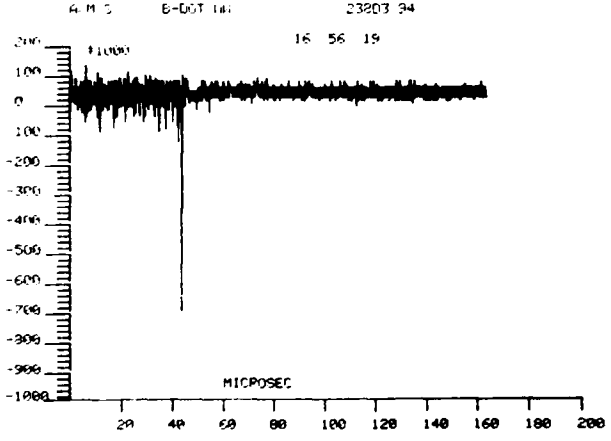

b. DTR Magnetic Field Derivative Record

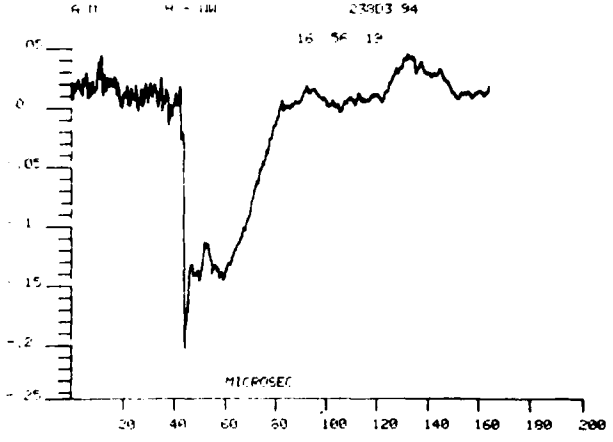

c. Magnetic Field (Integration of b.)

Figure 16. DTR Magnetic Field Waveforms Showing a Subsequent Return Stroke

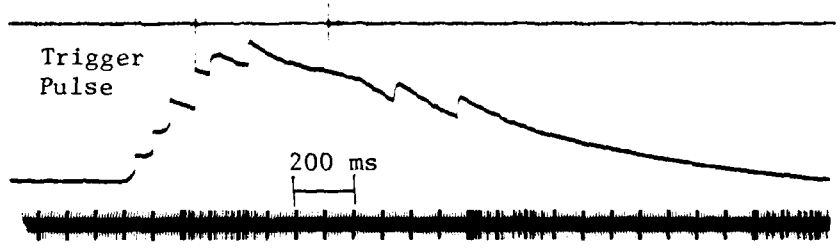

a. Analog Electric Field Record

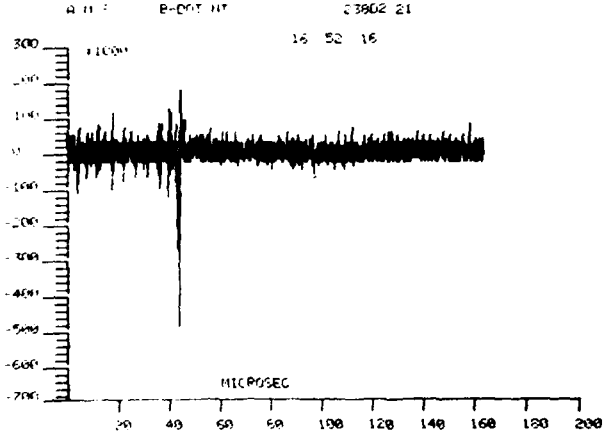

b. DTR Magnetic Field Derivative Record

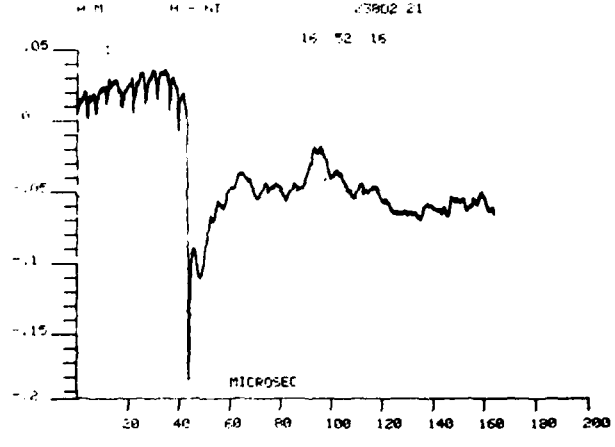

c. Magnetic Field (Integration of b.)

Figure 17. DTR Magnetic Field Waveforms for a Subsequent Return Stroke Preceded by a Dart-Stepped Leader

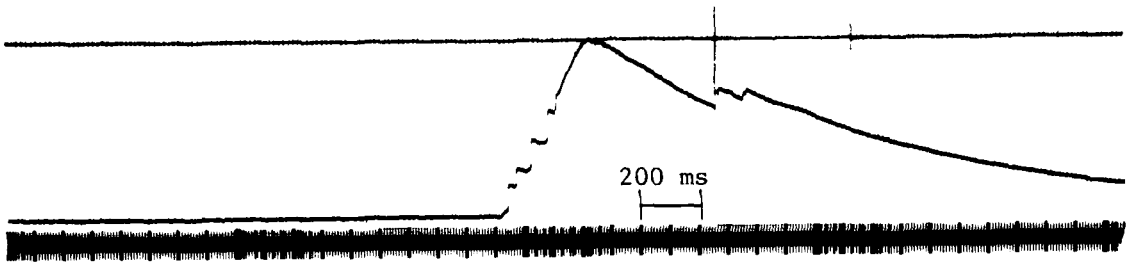

a. Analog Electric Field Record

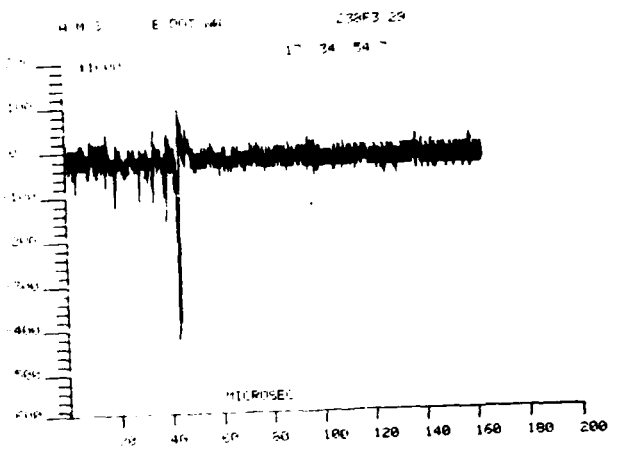

b. DTR Magnetic Field Derivative Record

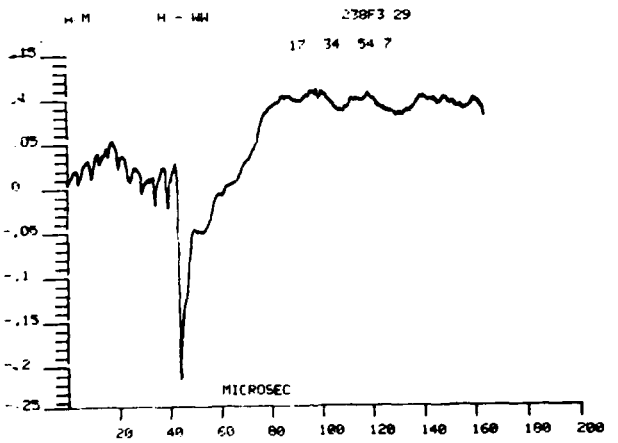

c. Magnetic Field (Integration of b.)

Figure 18. DTR Magnetic Field Waveforms for a Subsequent Return Stroke Preceded by a Dart-Stepped Leader

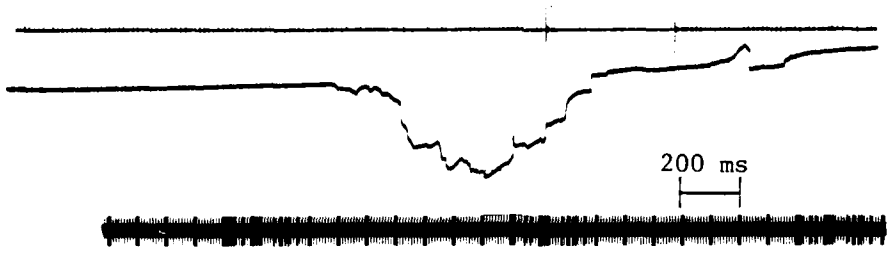

a. Analog Electric Field Record

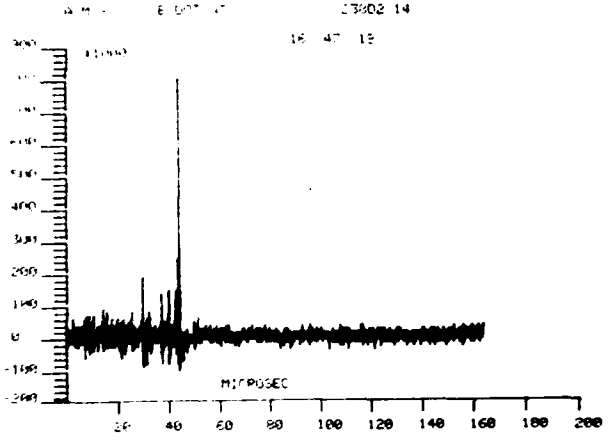

b. DTR Magnetic Field Derivative Record

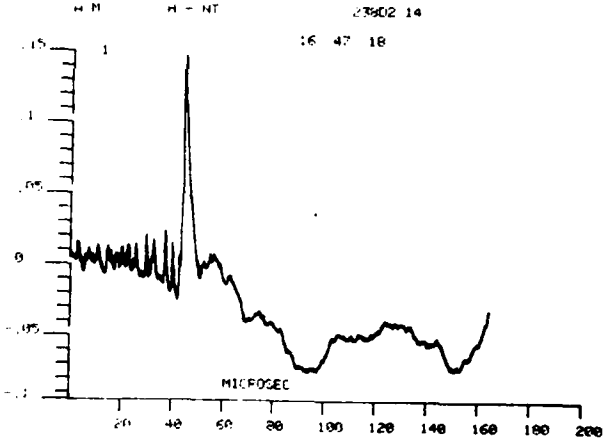

c. Magnetic Field (Integration of b.)

Figure 19. DTR Magnetic Field Waveforms for a Subsequent Return Stroke Preceded by a Dart-Stepped Leader

beginning of the return stroke. These return strokes are probably initiated by a dart-stepped leader although the DTR pretrigger interval does not appear to be sufficient to differentiate dart and stepped portions of the leader.

Uman et al. have developed theory that predicts similarities between ground level and above ground lightning electromagnetic fields for distant return strokes (Reference 8). From a comparison of simultaneous ground and airborne electric field measurements this prediction appears to be supported (Reference 4).

For positions close to lightning return stroke channels Uman et al. have calculated electromagnetic fields that vary considerably with altitude and distance. Examination of the analog electric field record revealed 33 flashes showing a stepped electric field change characteristic of a cloud-to-ground discharge but with a polarity opposite that normally produced by ground flashes. Radar data from the time of these flashes indicated that the aircraft was operating in close proximity to a thunderstorm. One example is shown in Figure 20. The slow leader electric field change preceding the first return stroke shows an initial rise similar to leader electric field changes for distant flashes followed by a field reversal and a return stroke field change of the opposite polarity. The DTR trigger pulse plotted in Figure 20 marks the time of initiation of the first return stroke. Ground based electric field data from this flash indicated that it was a negative cloud-to-ground discharge. Examination of the magnetic field polarities from the two aircraft magnetic field sensors and radar data from the time of the flash also indicated that the return stroke current was of the conventional polarity.

Wide bandwidth DTR data acquired at the time of the trigger pulse in Figure 20 is plotted in Figure 21. While the magnetic field waveshapes appear similar to those from other flashes, the electric field measured on the aft lower fuselage surface produced an unusual

waveshape as shown in Figure 21c. The electric field waveform shows an initial negative peak, the polarity typically produced at this sensor for cloud-to-ground flashes, followed by a gradual climb to a positive field level. Uman et al. have calculated and plotted electric fields for both the slow leader electric field change and for the first return stroke field change. Comparing the fields plotted in Figures 20 and 21 with the fields generated by Uman et al. it appears that the measurements closely correspond to fields predicted at an altitude of 5 km and a distance of 3 km for both the leader and return stroke. This position is within the thunderstorm range estimated from the airborne weather radar data.

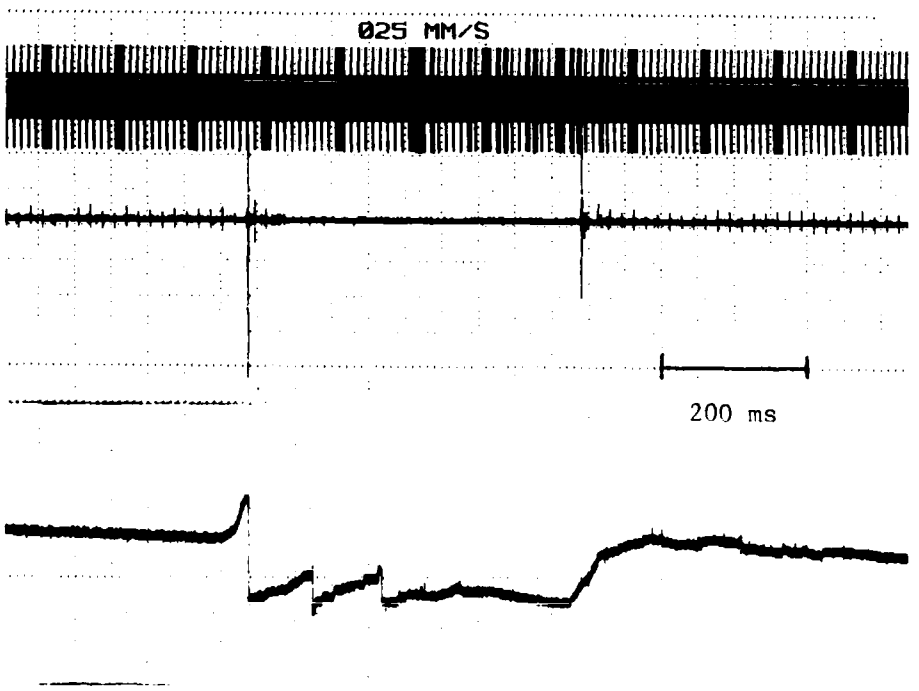

Figure 20. Electric Field Record of a Multistroke Cloud-to-Ground Flash with Reversed Polarity

b. Pre-Return Stroke Data

Sixty-eight digital records were obtained at varying times ahead of first return strokes on cloud-to-ground flashes. These records contained data from three separate phases of the discharge as indicated by categories a, b and c in Table 4. Additionally, recordings triggered by first return strokes contained 40 μs of pretrigger data also applicable to category c, stepped leader pulses.

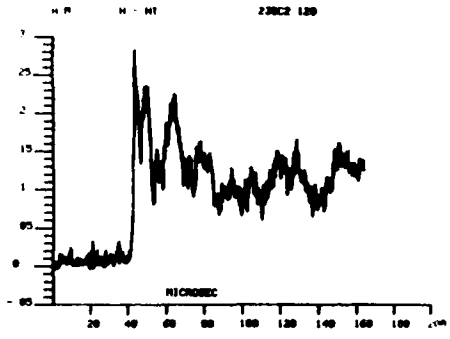

a. Wing Axis Magnetic Field Component

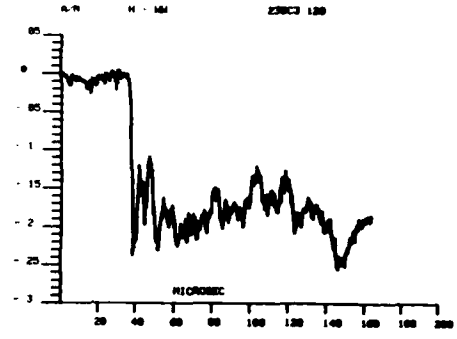

b. Fuselage Axis Magnetic Field Component

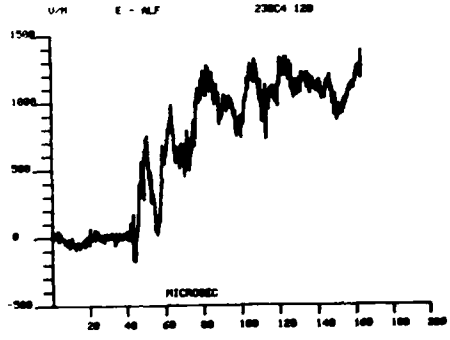

c. Electric Field Measured on the Aft Lower Fuselage Surface

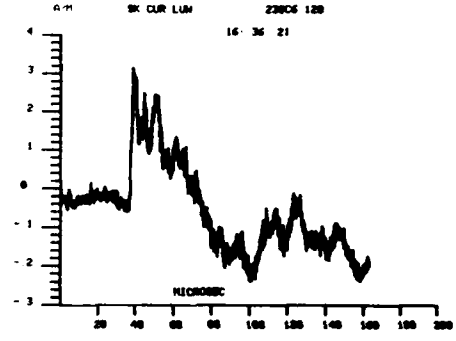

d. Skin Current on the Left Upper Wing Surface

Figure 21. DTR Electromagnetic Field Records for the First Return Stroke Shown in Figure 20

Beasley et al. have performed a study of the electric fields that precede cloud-to-ground flashes (Reference 19). They were able to identify three phases of pre-return stroke breakdown: preliminary electric field variations, characteristic pulses, and the stepped leader. The characteristic pulses (referred to as preliminary breakdown pulses by other researchers and in this report) marked the transition between the initial electric field changes and the stepped leader electric field changes. The pulses were usually 20 to 100 μs wide and occurred at 30 to 200 μs intervals. In the majority of cases the WC-130 analog electric field data were not reproduced with sufficient detail to resolve the small electric field changes of the preliminary variations or the relatively narrow pulses of the preliminary breakdown. It was difficult, therefore, to relate precisely the digital records obtained ahead of the return stroke to a specific phase of the pre-return stroke breakdown without further data processing. The waveforms could be divided, however, based on waveshape and time of occurrence relative to the apparent start of the stepped leader and the time of the first return stroke.

Digital records obtained within 10 ms of the return stroke contained multiple pulses with various amplitudes, waveshapes and durations. The larger pulses were mostly unipolar with pulse widths of 1 to 5 μs and times between pulses of 1 to 10 μs. Between the larger pulses there were a number of smaller pulses with similar characteristics. Based on the position of the DTR records relative to the return stroke and the shape and frequency of the larger pulses, it is assumed that the pulses were produced by leader steps (Reference 20). Examination of the pretrigger data from return stroke records shows that the large pulses became more distinctive closer to the time of the return stroke. Approximately 180 return stroke records showed very clear leader pulses. Assuming five or six leader pulses in each 40 μs pretrigger interval would give about 1000 pulses useful for further analysis. These records have an advantage in the fact that triggering was on the return stroke and not on the leader pulses, eliminating any direct bias in resulting statistics due to trigger system levels or characteristics.

Successive expansion of the analog field data illustrates one stepped-leader record as shown in Figures 22 through 24. Figure 22 is an electric field record with a trigger pulse indicating the location of a digital record just ahead of the first return stroke for a multistroke flash 38 km off the nose of the aircraft. Figure 23 is a plot of the analog magnetic field and time code with the trigger pulse marking the start of the digital record 0.25 ms ahead of the first return stroke. Leader pulses of increasing magnitude are evident in the magnetic field record from the trigger time up to the first return stroke. The overall 164 μs digital record for the magnetic field is finally shown in Figure 24. The abundance of pulses is evident in expanded waveforms to the right and at the bottom of the figure.

Leader pulses directly preceding a return stroke can be seen in Figures 10 through 12 for first return strokes and Figures 17 through 19 for subsequent strokes. Stepped leader pulses just ahead of subsequent strokes are closer together than those just ahead of first return strokes (approximately 4 μs between pulses) and appear less random in amplitude and waveshape.

The magnetic field records in Figures 24b and 11c illustrate some of the difficulties in identifying leader pulses from electromagnetic field measurements and the corresponding difficulty in establishing time intervals between leader pulses. Krider et al. (Reference 20) found leader pulse intervals of 16 μs ahead of first return strokes and 6.5 μs ahead of subsequent strokes. The example of Figure 24 shows much more frequent pulses for a first return stroke. From the expansion in Figure 24b the pulses encompass an amplitude range of 6:1, a range of pulse widths of 3:1, and a range of pulse intervals of 6:1. It is not clear that all of these pulses should be considered leader steps. Photographic studies seem to confirm the longer intervals of Krider et al. Some of the data of Krider also shows frequent pulses of smaller amplitude between identified leader steps although these pulses are not discussed. The fact that some lightning discharges produce relatively frequent pulses during the leader such as the example in Figure 24, while others produce less frequent, more distinct, uniformly spaced

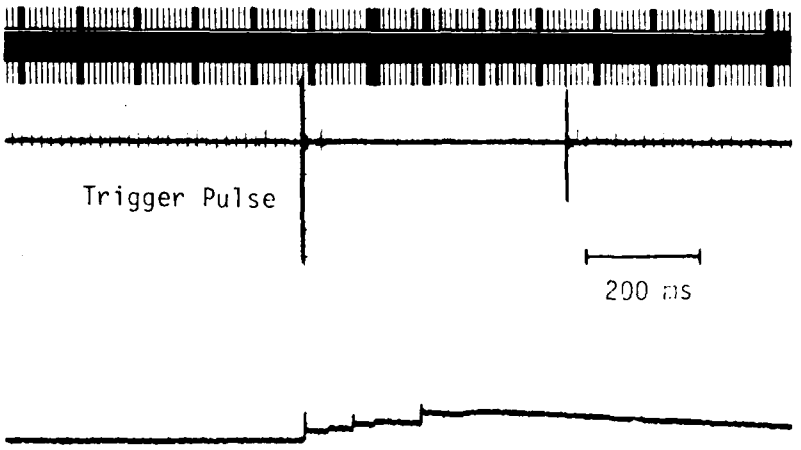

Figure 22. Electric Field Record for a Cloud-to-Ground Flash with a DTR Trigger Pulse 250 μs Prior to the First Return Stroke

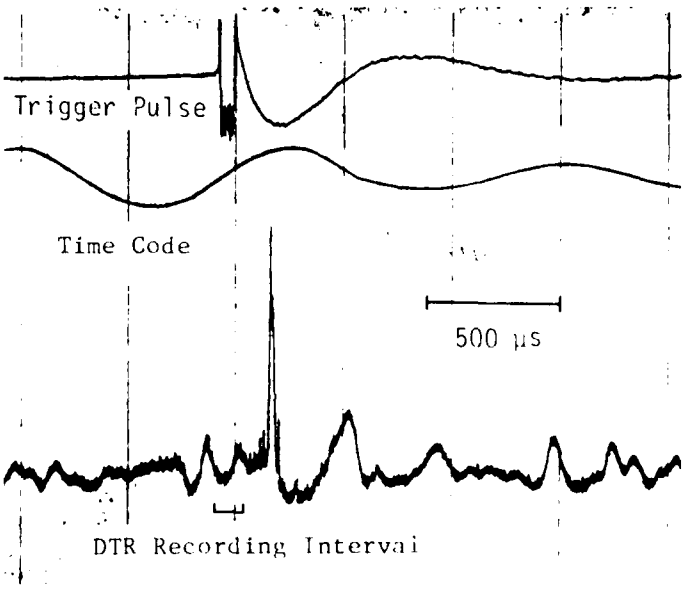

Figure 23. Analog Magnetic Field Record with DTR Trigger Pulse for the Flash Shown in Figure 22

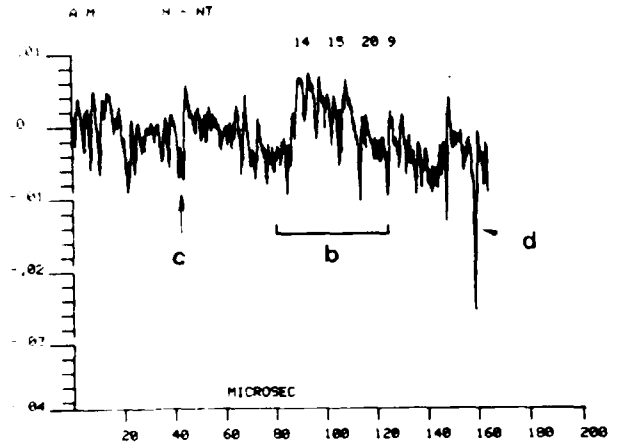

a. 164 μs Magnetic Field Record

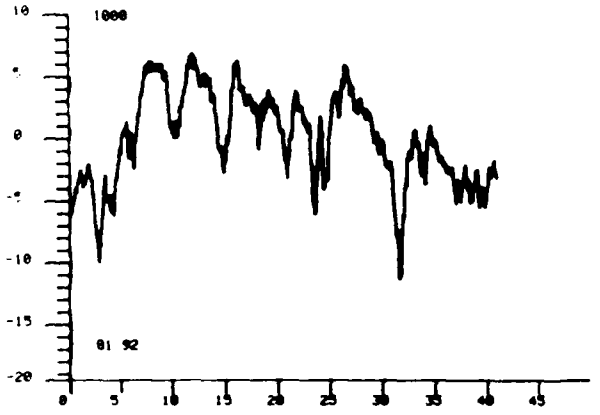

b. 40 μs Interval from Bracketed Section in a.

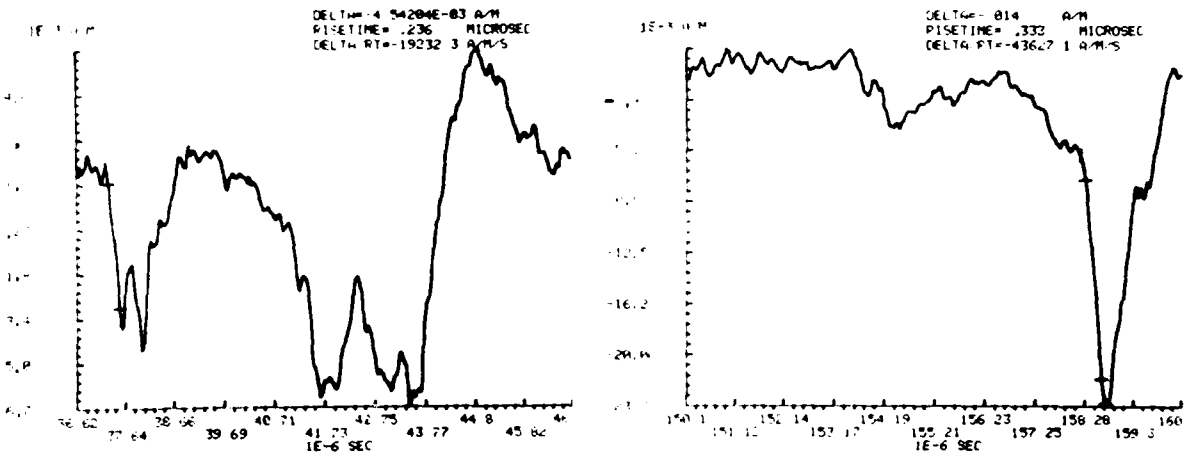

c and d. 10 μs Expansions from a. Showing Risetimes

Figure 24. DTR Magnetic Field Records Showing Leader Pulses from the Flash in Figure 23

leader pulses, such as in Figure 10c, may be due to multiple branches or other breakdown processes developing simultaneously in some flashes.

Records obtained near the beginning of the leader process exhibited pulses typical of those shown in Figure 25. The largest pulses were usually bipolar with a slow concave front, a fast transition to peak, and a slower decay through zero with a small amount of overshoot. Superimposed on the rising front of the waveform were several small, narrow, unipolar pulses.

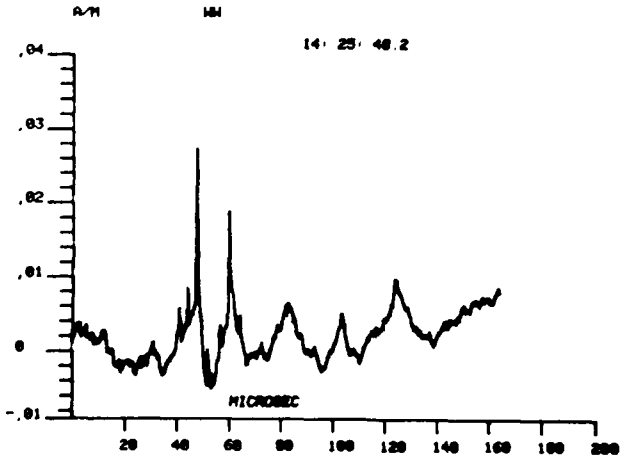

Figure 25. Preliminary Breakdown Pulses

The decay following the peak of each pulse was occasionally smooth but more often had one or two small unipolar pulses superimposed on the decaying waveform as shown in Figure 25. Pulse widths were 10 to 25 μs at the base of the large pulses and around 1 μs for the smaller pulses. The large pulses most frequently occurred in pairs separated by 10 to 25 μs and were occasionally followed by one to three smaller, slower pulses as shown in Figure 25. These waveforms are similar to those measured by Weidman and Krider at the end of preliminary breakdown (Reference 20). Eleven records containing this type of data were obtained 10 to 33 ms prior to the first return stroke with an average of 18 ms. This is comparable to the average stepped leader durations found by Beasley, which would be expected if the pulses occurred during the

period of characteristic pulses used by Beasley to separate the preliminary variations from the start of the stepped leader. Another example is shown in Figures 26 and 27. Figure 26a shows the overall electric field and trigger pulse location for a multistroke flash approximately 13 km from the aircraft. An expansion of the electric field (Figure 26b) shows a trigger pulse 11.5 ms ahead of the return stroke at the beginning of the leader electric field change. Also shown in the expansion are the two axis analog magnetic fields with an arrow marking the magnetic field that coincides with the trigger time. The digital record obtained at this time is shown in Figure 27a with expansions in Figure 27b.

The greatest percentage (71%) of pre-return stroke data consisted of fast narrow pulses occurring before the stepped leader electric field change. The pulses appeared most frequently in pairs and also singly or in groups of three or four with 5 to 100 μs between pulses as shown in Figure 28. Pulse risetimes were very fast, typically on the order of 100 ns and occasionally approaching the limit of the recording system time resolution (40 ns). Pulse widths varied from 150 ns to several microseconds. These pulses were reported by Rustan in Reference 4 for several flashes with simultaneous airborne and ground field measurements. Some of the data shown by Weidman and Krider in Reference 21 may be from similar pulses.

A distribution of time intervals from DTR trigger to first return stroke for these pulses is shown in Figure 29. The longest interval was 110 ms and the average interval was 36.7 ms. These times fall within the range found by Beasley for the preliminary variation phase of the discharge. The narrow pulses do not necessarily occur only in the early phases of cloud-to-ground discharges. Similar pulses appear superimposed upon and interspersed between the larger pulses of the preliminary breakdown DTR records as can be seen in Figures 25 and 27. Other narrow pulses occur at various times throughout intracloud discharges. Pulses occurring later in the flash would be less likely to be captured by the DTR because other signals such as preliminary

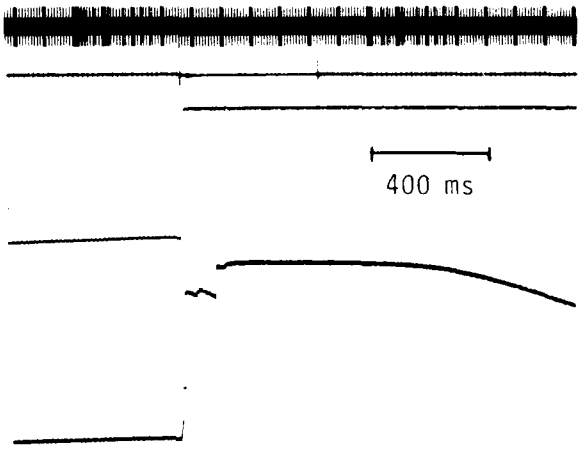

a. Electric Field Records

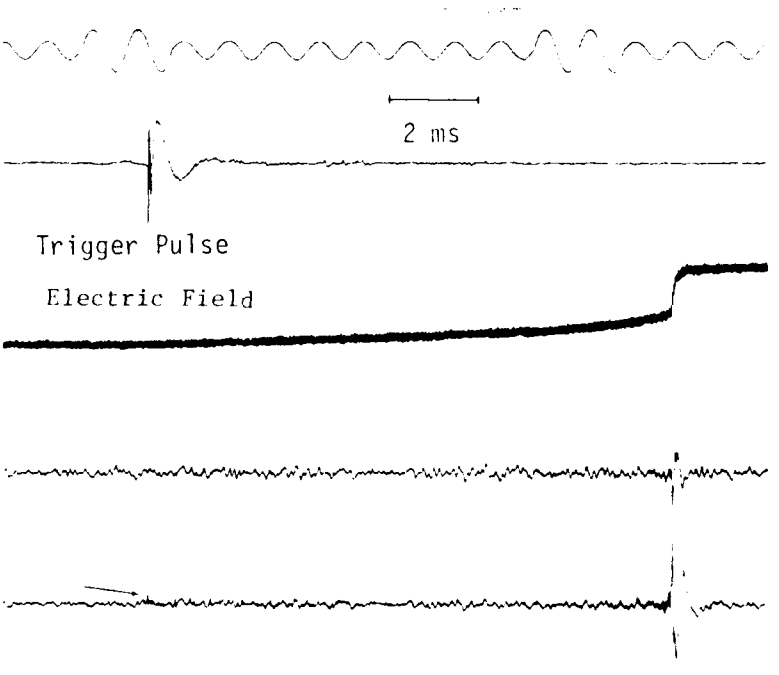

b. Magnetic Field Records

Figure 26. Analog Electric and Magnetic Field Record with a DTR Trigger Pulse at the Beginning of the Leader Process

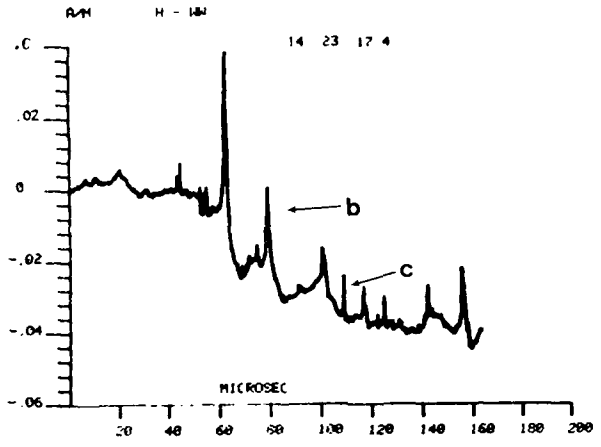

a. 164 μs Magnetic Field Record

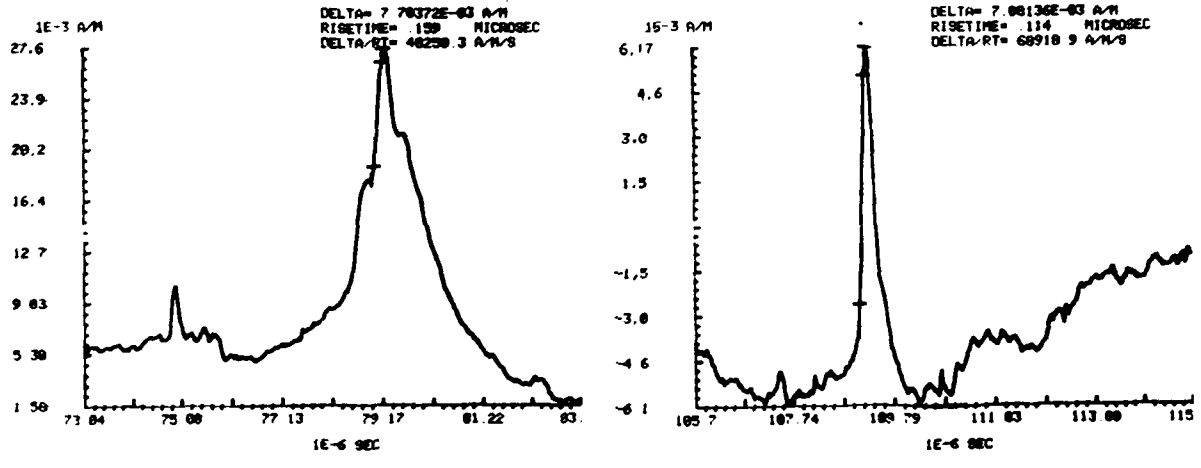

b. and c. 10 μs Expansions from a.

Figure 27. DTR Magnetic Field Record Obtained at the Beginning of the Stepped Leader Process from the Flash in Figure 26

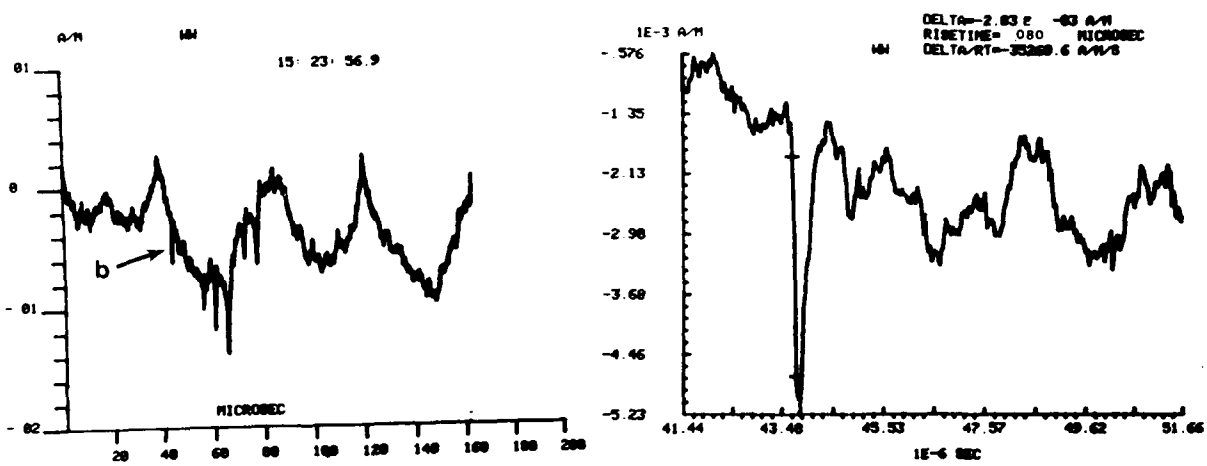

a. Magnetic Field

b. First Pulse - Expanded

Figure 28. DTR Magnetic Field Records of Pulses Occurring Before the Stepped Leader Electric Field Change

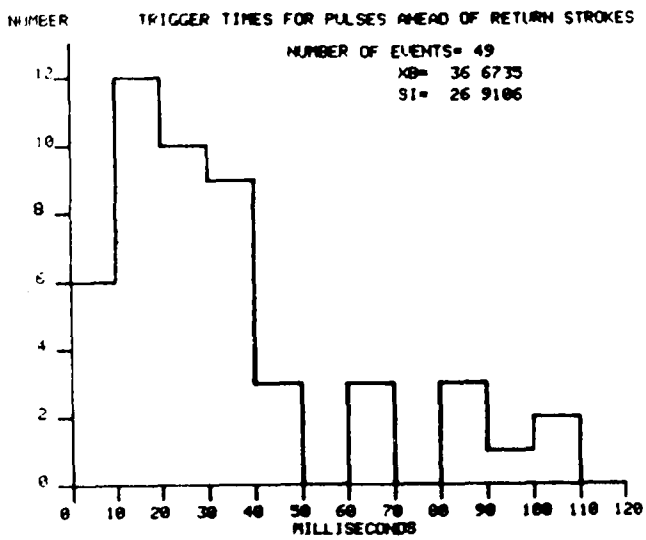

Figure 29. Distribution of Time Intervals from DTR Trigger to First Return Stroke for DTR Records of Pre-Leader Pulses

breakdown pulses, stepped leader pulses or return strokes would trigger the recording system, disabling it until the digital data was stored. A search of the analog record may uncover more pulses but most of them probably would not appear due to the narrow pulse widths and the 2 MHz recording bandwidth limitation. Examples of the waveforms are shown in Figures 30 through 33. Figures 30 and 31 are magnetic field records preceding cloud-to-ground flashes. Figures 32 and 33 show magnetic field records obtained during intracloud discharges.

Intracloud flashes produced electromagnetic field waveshapes with various characteristics on a microsecond time scale. As was mentioned above, fast narrow pulses were recorded at different times throughout intracloud discharges, often at the beginning of the slow electric field change. These pulses were similar to those measured prior to the leader on cloud-to-ground flashes. Examples are shown in Figure 32.

Electromagnetic field pulses, similar to those recorded at the end of preliminary breakdown during cloud-to-ground flashes and similar to those reported by Weidman and Krider during intracloud discharges (Reference 21), were recorded during several intracloud lightning flashes. Characteristics of these pulses have been described above. An example of one such record is given in Figure 34. Other intracloud pulses with more random waveshapes appeared singly or in groups as shown in Figure 35.

Often the discharges produced sequences of pulses as shown in Figure 36. Krider and Radda have reported sequences of regular radiation field pulses during intracloud lightning discharges in ground measurements (Reference 22). The airborne measurements appeared to be more random in waveshape, amplitude, pulse width and pulse spacing than the data of Krider and Radda. Similar pulse sequences occurred after return strokes in ground flashes as shown in Figure 37.

c. Electromagnetic Field Risetimes

Electromagnetic field risetimes can be shown to be related to the risetime of the current pulse producing the field (Reference 23). The

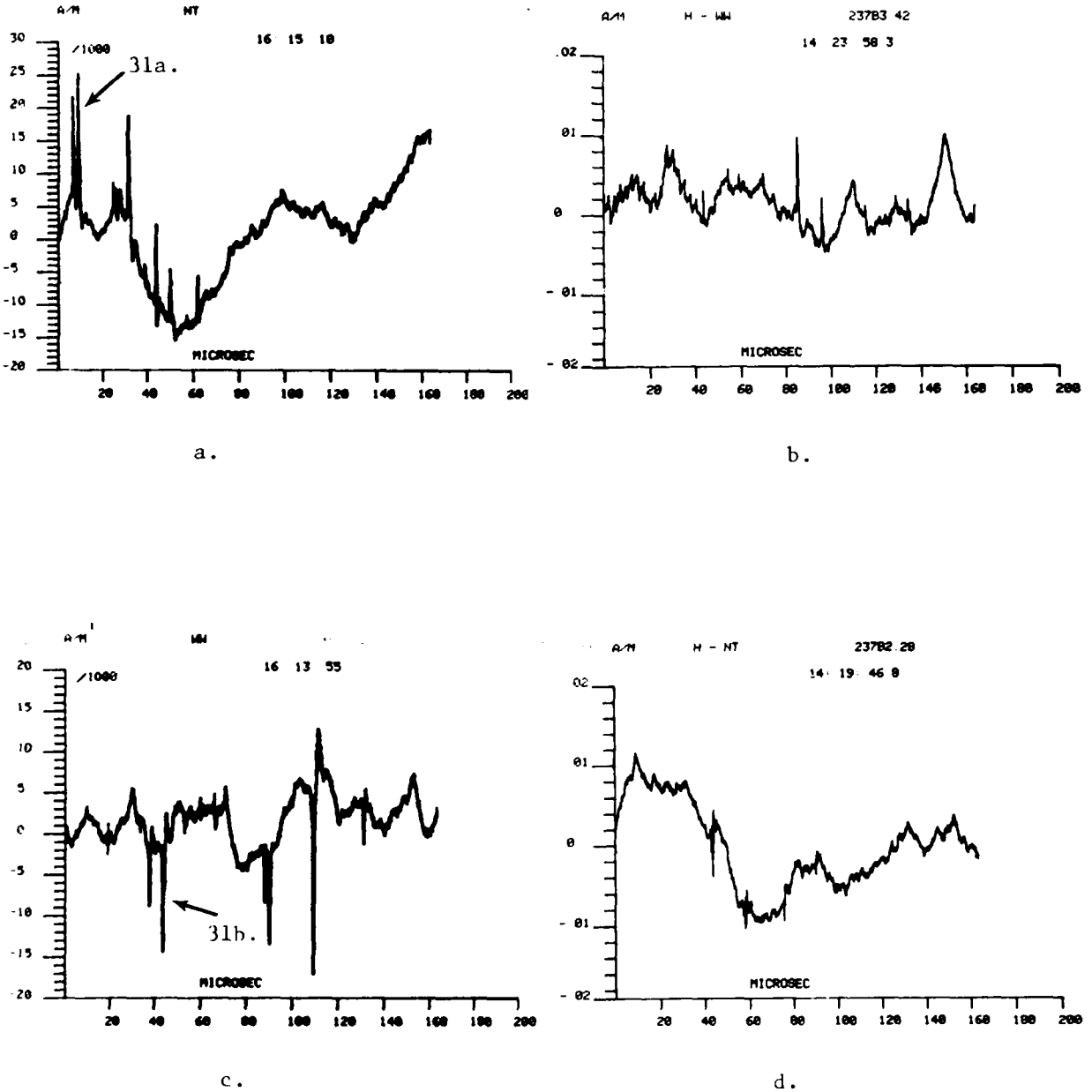

a. b.

c. d.

Figure 30. DTR Magnetic Field Records Showing Pre-Leader Pulses

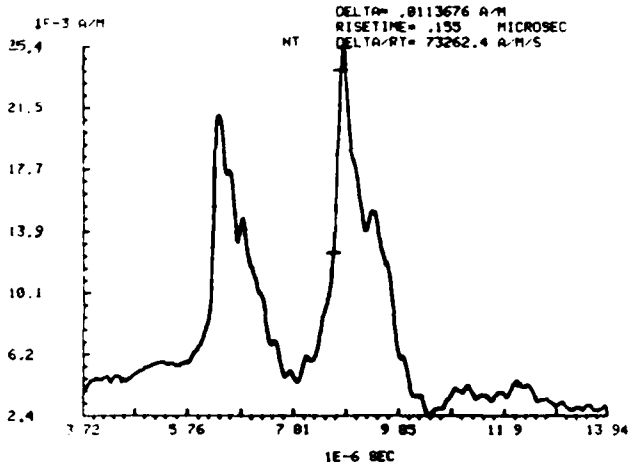

a. 10 μs Expansion from Figure 30 a.

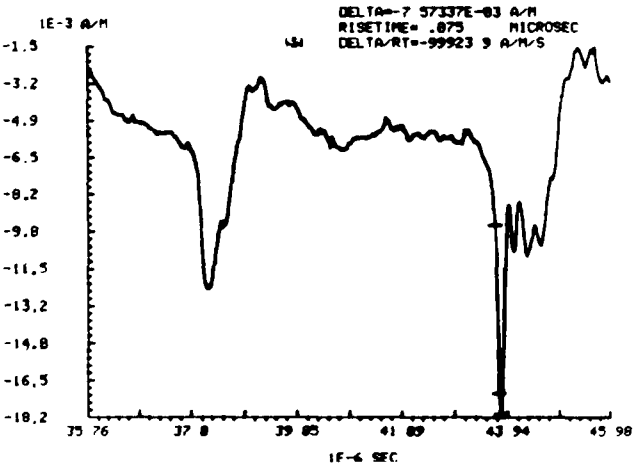

b. 10 μs Expansion from Figure 30c.

Figure 31. Expanded Plots of Pre-Leader Pulses from Figure 30

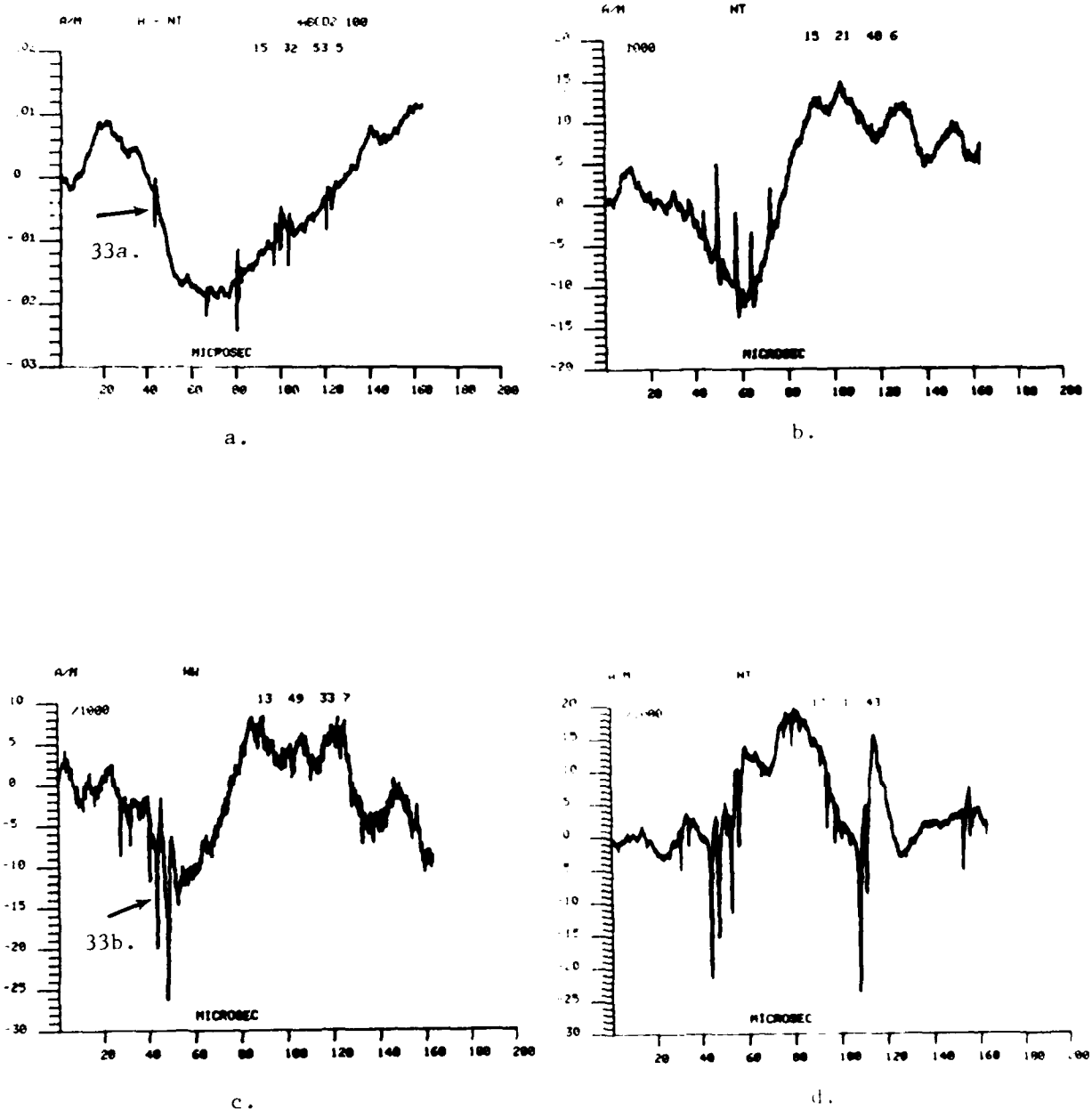

a. b.

c. d.

Figure 32. DTR Magnetic Field Records Showing Narrow Pulses from Intracloud Flashes

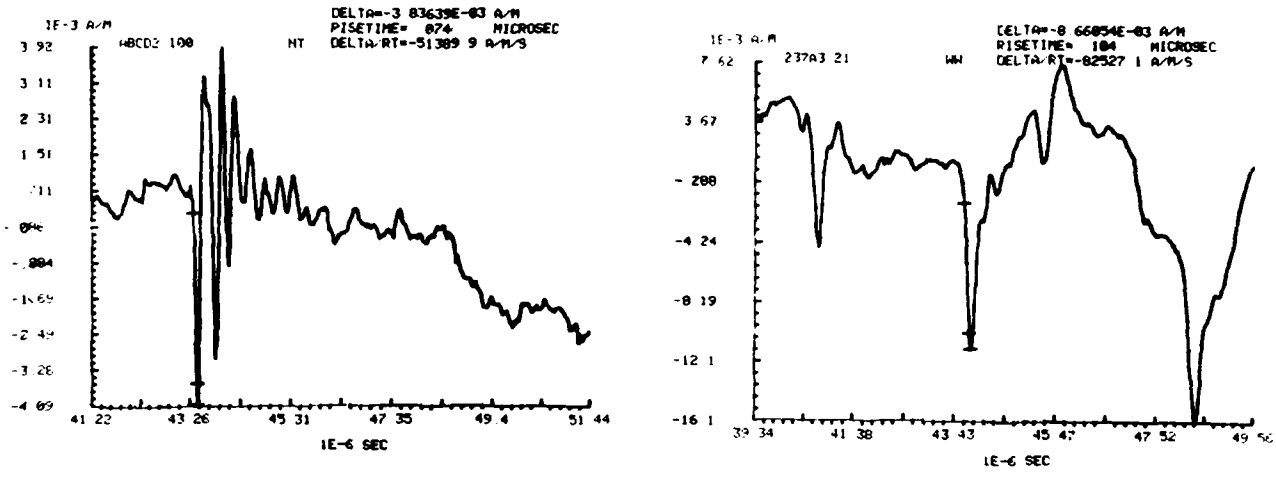

a. 10 μs Expansion from Figure 32a.

b. 10 μs Expansion from Figure 32c.

Figure 33. Expanded Plots of Intracloud Pulses from Figure 32

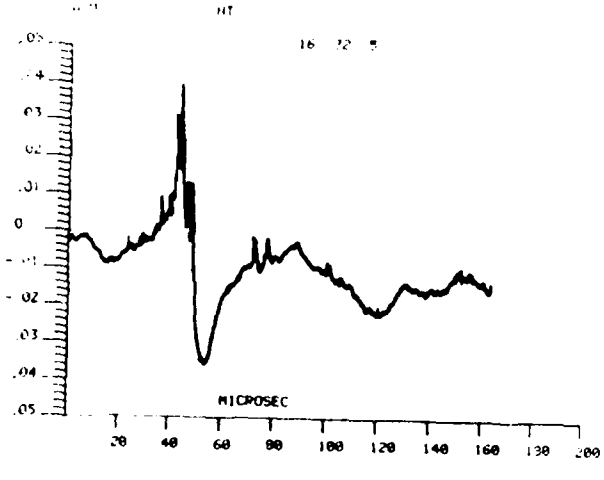

Figure 34. DTR Magnetic Field Record of a Bipolar Intracloud Pulse

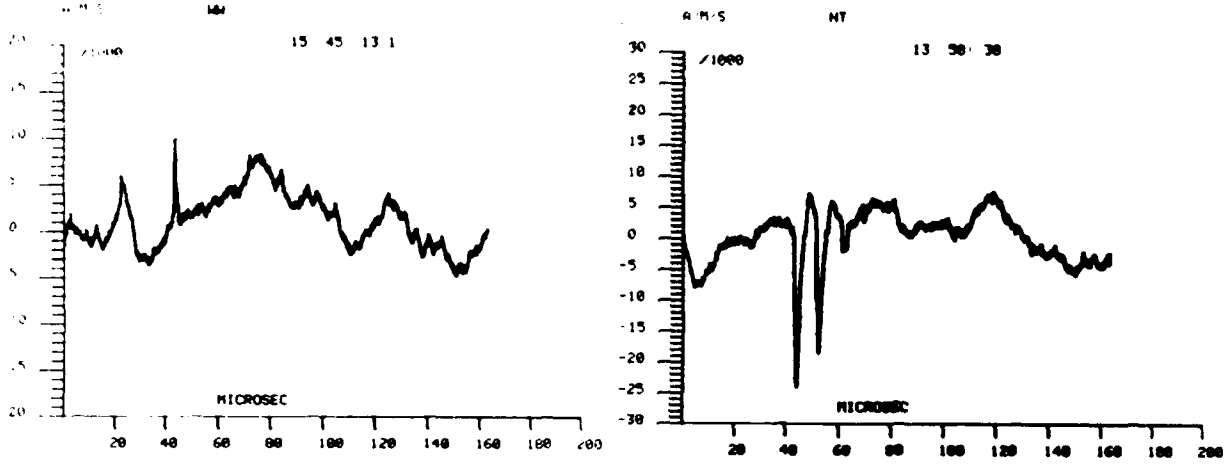

a. b.

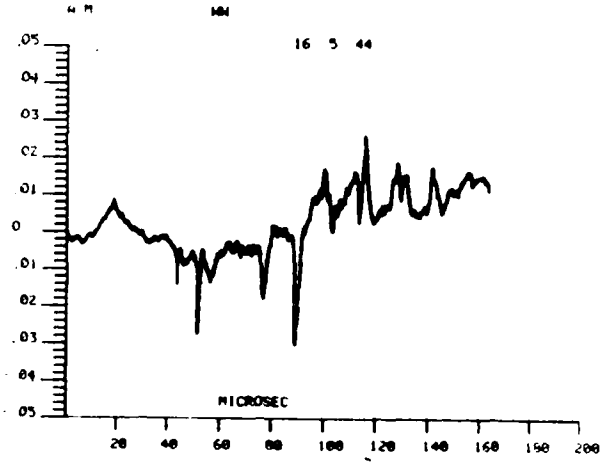

c.

Figure 35. DTR Magnetic Field Redords Showing Intracloud Discharge Pulses

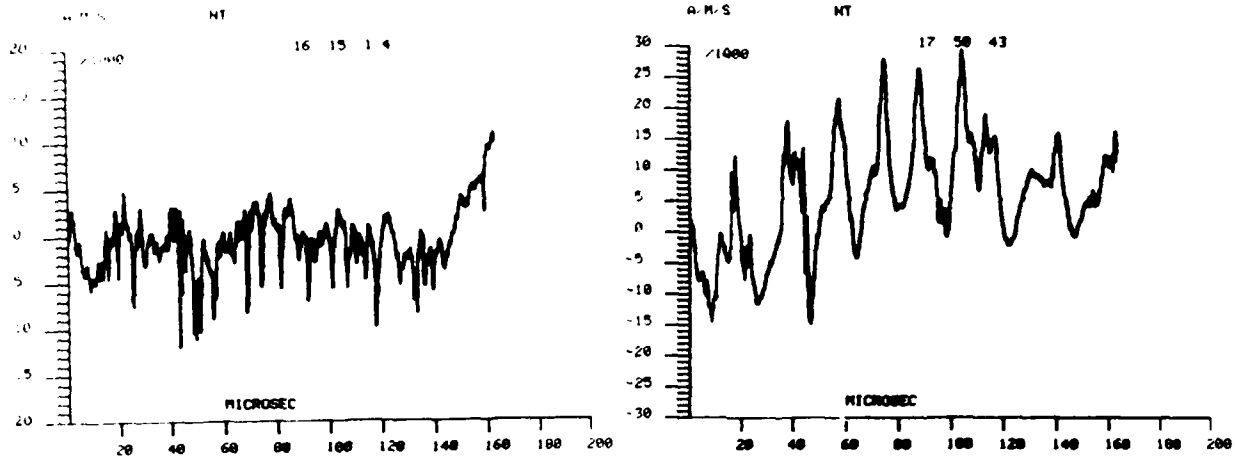

a. b.

Figure 36. DTR Magnetic Field Records of Pulse Sequences During Intracloud Flashes

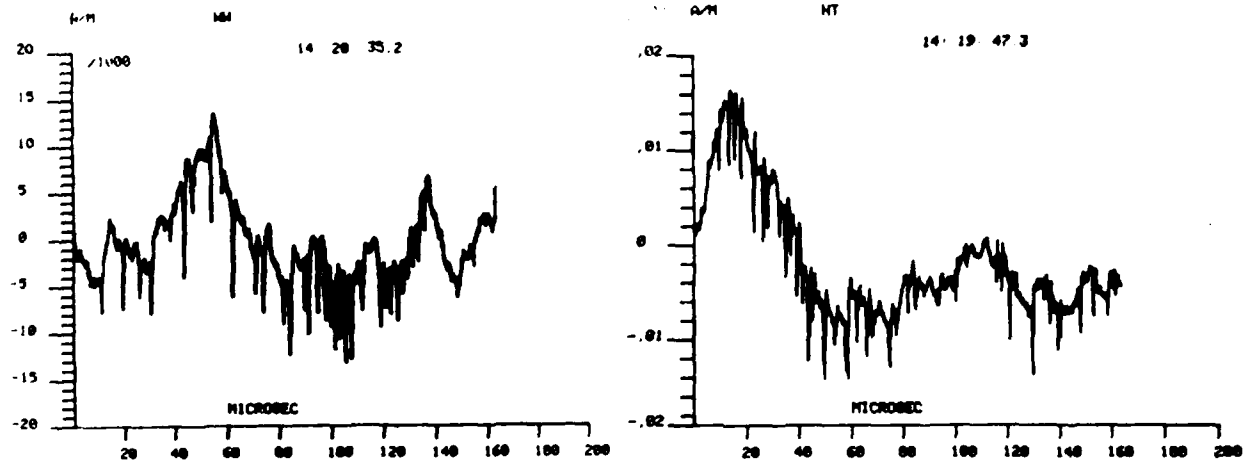

a. b.

Figure 37. DTR Magnetic Field Records of Pulse Sequences During Cloud-to-Ground Flashes

field or current risetime gives an indication of the severity of the induced coupling hazard to aircraft systems. Lightning waveforms often have complex shapes on the rising front of the waveform. In the case of the return stroke, the waveform is composed of a slowly increasing concave portion followed by a fast, more linear rise to peak. Risetimes reported in the literature have been determined from the 10% to the 90% point over the entire front of the waveform with the slow portion included and also just over the fast transition (References 12 and 24). Risetimes for the fast transition are a more meaningful parameter in estimating electromagnetic hazards and therefore fast transition risetimes are used in the following discussion.

Two factors are expected to affect the high frequency characteristics of distant airborne lightning measurements. For electromagnetic fields originating near ground level, such as a return stroke, the wave must propagate over an imperfectly conducting surface, leading to attenuation of high frequency components in the wave (Reference 25). Once the wave reaches the aircraft where the measurement is performed, electromagnetic interaction with the aircraft structure further distorts the characteristics of the waveform. For lightning discharges which occur far above ground, such as some leader steps and intracloud discharges, the propagation path to the aircraft is more direct and should result in less high frequency attenuation. Certain sensors and sensor placements on the aircraft decrease distortion due to aircraft interaction. For the risetime measurements presented below, signals from the B-dot sensor sensitive to magnetic fields in the direction of the fuselage axis were used. The orientation and position of this sensor is expected to produce less distortion in the measured electromagnetic fields (Reference 26 and 27).

Risetimes for return stroke electromagnetic fields have been previously calculated for airborne WC-130 measurements and reported in References 4 and 12. Risetimes for the fast portion of the return stroke waveform ranged from 100 ns to 900 ns with an average of 356 ns for first strokes and 100 ns to 800 ns with an average of 405 ns for

subsequent strokes. Maximum current rates of rise were estimated to range from 5.8×10^9 amperes/second (A/s) to 1.03×10^{11} A/s.

Other lightning discharge processes often produced risetimes shorter than return stroke risetimes. Risetimes were calculated for all the categories of digital data listed previously. Nine to 17 pulses from each category were selected at random for risetime analysis. Magnetic field amplitudes and rates-of-change were also calculated from 16 additional large pulses and 14 additional narrow pulses from discharges occurring above ground where the storm could be identified on radar displays.

Magnetic field risetimes are summarized in Table 5. The shortest risetime, 49 ns, was produced by a small unipolar pulse superimposed on the larger field change of a preliminary breakdown pulse. The shortest average risetime was 122 ns resulting from pulses occurring before the stepped leader on cloud-to-ground flashes. Risetimes for leader pulses were calculated from pulses occurring just ahead of the return stroke (less than 40 μs ahead). Average stepped leader and dart-stepped leader pulse risetimes were 294 and 277 ns respectively, approximately twice the risetimes of small pre-return stroke pulses. The longest average risetime was produced by large preliminary breakdown pulses with an average risetime of 435 ns. Field changes for all these data, with the exception of the large preliminary breakdown pulses, were two to four times faster than field changes occurring during the return strokes reported by Rustan et al. (Reference 11).

Although the field changes occurred more rapidly in most non-return stroke discharges, the field changes were often small. To determine relative electromagnetic hazard levels between these pulses and return stroke data, magnetic field characteristics from 30 pulses were normalized to 100 km and compared to normalized ground-based and airborne lightning measurements. Range was determined from airborne radar displays as described previously. Normalizing was performed assuming field intensity is inversely proportional to distance. The altitude of the discharges was taken to be the same as that of the

TABLE 5

LIGHTNING ELECTROMAGNETIC FIELD RISETIMES

Category	Sample Size (Pulses)	Risetime (ns) min	max	avg
a) Pulses Preceding Stepped Leader Electric Field Changes	10	56	245	122
b) Preliminary Breakdown Pulses				
Large Pulses	12	117	1700	435
Small Pulses	9	49	309	134
c) Stepped Leader Pulses				
Before 1st Return Stroke	11	138	740	294
Before Subsequent Strokes	11	145	423	277
d) First Return Strokes*	128	100	900	356
e) Subsequent Return Strokes* Preceded by a Dart Leader	71	100	800	405
f) Subsequent Return Strokes Preceded by a Dart-Stepped Leader	not analyzed			
g) Pulses after the First Return Stroke in Cloud-to-Ground Flashes	11	165	596	249
h) Narrow Pulses during Intracloud Discharges	17	75	386	172
Overall	280	49	1700	335

* Return Stroke Data are from Reference 12

aircraft (approximately 5 km). Since the discharges occurred beyond 10 km the errors due to this assumption may result in underestimates of up to 30%. Lightning channel orientations were assumed to be such that the magnetic fields produced were fully coupled into the magnetic field sensors, an assumption that may also lead to underestimates in the magnetic fields. Magnetic field rates-of-change were taken directly from the measurements and normalized while corresponding field transitions were obtained by integrating the data and normalizing.

Sixteen pulses, four ahead of first return strokes and twelve from intracloud flashes, produced normalized magnetic field rates-of-change ranging from 2.8×10^3 amperes/meter/second (A/m/s) to 2.9×10^4 A/m/s with an average of 1.4×10^4 A/m/s. Normalized field transitions over the fast part of the waveform ranged from 4.3×10^{-4} A/m to 2.8×10^{-3} A/m with an average of 1.5×10^{-3} A/m. For seven narrow pulses occurring ahead of first return strokes and seven narrow pulses occurring during intracloud discharges, normalized magnetic field rates-of-change ranged from 4.9×10^3 A/m/s to 2.0×10^4 A/m/s with an average of 9.4×10^3 A/m/s. Normalized field transitions for the narrow pulses averaged 4.7×10^{-4} A/m with a range of 2.1×10^{-4} A/m to 1.1×10^{-3} A/m.

Using the return stroke data of Rustan et al. in Reference 11 and the equations used by Rustan to infer return stroke current rate-of-change, normalized magnetic field rates-of-change should range from 1.9×10^4 A/m/s to 5.5×10^4 A/m/s with an average of 2.4×10^4 A/m/s. Comparing return stroke results to the pulse data just presented would indicate that some large cloud pulses produce field rates-of-change approaching those from return strokes. The smaller pulses, while producing faster risetimes, have lower magnetic field rates-of-change.

Return stroke rates-of-change found by Rustan may be underestimated for two reasons. Field rates-of-change were determined by assuming a linear increase in field between the 10% and 90% points and dividing the 10% to 90% field transition by the corresponding risetime.

This technique can underestimate true rates-of-change as shown by Baum (Reference 28). Also, since the fields associated with the initial front of the return stroke are generated near ground level, some ground propagation is involved, possibly attenuating high frequencies and resulting in lower measured field rates-of-change. Fields generated well above ground such as those from intracloud discharges would not suffer the same effect.

Krider and Weidman have made ground-based electric field measurements of lightning over saltwater, conditions where propagation effects should be minimized (Reference 29). They found average return stroke electric field risetimes of 90 ns over the fast front of the waveform with a standard deviation of 40 ns. Electric field rates-of-change averaged 33 volts/meter microsecond (V/m/μs) with a standard deviation of 14 V/m/μs normalized to 100 km. Assuming distant electric and magnetic fields are related by the impedance of free space, the corresponding average magnetic field rate-of-change normalized to 100 km would be 8.8×10^4 A/m/s with a standard deviation of 3.7×10^4 A/m/s. This value is more than three times larger than the data reported by Rustan et al. (Reference 11).

Krider gives data for cloud pulses with a mean electric field rate-of-change of 16 V/m/μs at 100 km. Dividing by two to remove the image contribution present in ground fields (Reference 23), this value would correspond to a magnetic field rate-of-change of 2.1×10^4 A/m/s. This value is almost twice that found in the airborne measurements. Krider and Weidman show no data from cloud pulses slower than about 5 V/m/μs which corresponds to a magnetic field rate-of-change of about 6.5×10^3 A/m/s, while the airborne measurements clearly show data slower than this. On the other hand the fastest airborne data from cloud pulses is 2.9×10^4 A/m/s equivalent to 11 V/m/μs at 100 km which is slightly higher than the average value for the corresponding data of Krider and Weidman. Sample sizes from both sets of data are small so the differences may not be significant. Since the DTR data window was large, some of the cloud pulses that were used were not those that triggered the DTR. This may have resulted in the inclusion of some data too slow

or too small to trigger the recording system. If the trigger characteristics of the instrumentation used by Krider and Weidman were similar to that on the WC-130, these pulses would have been missed by Krider and Weidman, resulting in different statistics. It is interesting that the airborne cloud pulse characteristics more closely approximate the data of Krider and Weidman than do the return stroke characteristics, possibly due to the effects of ground propagation on the return stroke fields.

SECTION V

DISCUSSION

From a cursory examination of aircraft electric field data from the 25, 26, and 27 August 1981 research flights, it appears that the storms encountered were typical of Florida thunderstorms. Thunderstorm flashing rates were slightly higher on the average than usual but peak flashing rates were less than those of some intense Florida thunderstorms. The percentage of flashes that were intracloud was the same as that found by other researchers for Florida thunderstorms. The electric field displays were useful for identifying and correlating electric field and DTR data but were not sufficiently expanded to provide detailed information on any specific lightning flash.

Over 500 digital recordings of lightning electromagnetic fields were acquired over the three flight days, the majority on return stroke fields. If all the research flights were equally successful in recording lightning data, the total number of useful DTR acquisitions should be around 1500 records with over 1000 showing return strokes. Despite more frequent occurrence of intracloud lightning flashes, the majority of DTR recordings were triggered on cloud-to-ground discharges, an indication of the relative electromagnetic hazards of the two types of lightning. The fact that relatively threatening lightning discharges occur in cloud flashes less often than ground flashes may be counteracted in practice by the fact that the flight environment is the main environment of concern for aircraft protection, and aircraft lightning attachments from cloud discharges may occur more frequently than attachments during ground flashes. Airborne measurements of electromagnetic fields from distant lightning produced waveshapes very similar to those measured on the ground for many types of discharges reported in the literature. More detailed examination of the waveforms may reveal slight differences in the waveform structure due to the displaced position of the field measurement (i.e. above ground). For some close lightning, airborne electric field waveforms appeared to be inverted from the normal sense due to the position at which the measurement was made.

Derivative airborne magnetic field records of lightning stepped leaders and return strokes revealed a multitude of pulses occurring throughout the leader phase and after the initiation of the return stroke. Airborne measurements of pulse sequences occurring in the clouds also revealed a multitude of pulses of various amplitudes. Pulses occurring in the 100 μs period following the initiation of the return stroke produced magnetic field rates-of-change approaching those produced by the return stroke. Similar pulses were not present in subsequent strokes, suggesting that the pulses are from discharges outside the main return stroke channel. Such discharges are of interest since the pulses are fast and more numerous than return strokes and thus present a potential threat to aircraft. Over 100 DTR recordings of narrow unipolar pulses were recorded prior to ground strokes and during intracloud flashes. These pulses produced the fastest observed risetimes but were of small amplitude. Average risetimes from all the DTR data were in the submicrosecond range extending from 122 ns for the pulses just mentioned to 435 ns for large cloud pulses with an overall average of 335 ns. The risetimes are all substantially lower than risetimes presently used to define standard lightning threat levels (Reference 30). The implications of this waveform feature remain to be evaluated. Magnetic field rates-of-change were highest for return strokes but larger cloud pulses produced field rates-of-change approaching return stroke levels. Ground based measurements of return stroke fields over saltwater showed shorter average risetimes and higher field rates-of-change than the airborne measurements. Ground propagation is the possible cause of the high frequency attenuation of the airborne return stroke fields. Cloud pulses measured at the aircraft show field rates-of-change close to rates from cloud discharges over saltwater measured on the ground. Sequences of pulses during cloud discharges are of concern not only because of the potentially high field rates-of-change and corresponding current rates-of-change but also because of the repetitive nature and long duration of the discharges.

SECTION VI

CONCLUSIONS

We have performed a review of the lightning data recorded on a NOAA WC-130 aircraft during the summer of 1981. The data are recorded on fifty-eight 15 minute analog tapes containing 6143 digital data files. Detailed review of data from the last three flight days revealed 1034 lightning flashes in the analog record with 518 identified digital recordings. Three hundred and forty seven digital records were return strokes, 68 records were from fields ahead of the first return stroke and 97 records were from fields from intracloud lightning discharges. The majority of DTR data was triggered during ground flashes despite the fact that more lightning discharges were intracloud, an indication of the relative frequency of threatening discharges present in the two types of lightning.

All of the DTR records obtained on the last three flight days have been viewed and processed. Records containing pertinent data have been integrated, plotted and classified. Preliminary risetime calculations have been made for each category of digitally recorded electromagnetic field data. Risetimes for the fast field changes of return strokes have been obtained previously and are on the order of 400 ns. Risetimes for other discharge pulses ranged from about 100 ns to about 400 ns. Nearly 50 DTR records acquired just before lightning stepped leaders showed single or multiple unipolar pulses with narrow pulse widths and risetimes down to 40 ns. These results bear out the findings of recent years that large submicrosecond components exist in many lightning processes and identify two processes that perhaps warrant greater interest -- pulses produced after initiation of the first return stroke and pulses occurring in the initial phases of intracloud and cloud-to-ground flashes.

Magnetic field rates-of-change were estimated for several types of discharges and compared to ground-based measurements over saltwater. Rates-of-change were 9.4×10^3 A/m/s for small cloud pulses and

1.4×10^4 A/m/s for large cloud discharge pulses normalized to 100 km. Average return stroke magnetic field rates-of-change were estimated to be 2.4×10^4 A/m/s normalized to 100 km although these data appear to be attenuated by ground propagation. Data from ground measurements over saltwater showed field rates-of-change two to three times higher than the airborne measurements, perhaps due to different trigger characteristics in the respective data acquisition systems. Magnetic field rates-of-change associated with leader pulses and pulses immediately following the initial return stroke peak averaged 0.3 and 0.4 times the return stroke rate-of-change respectively. Some pulses occurring less than 100 μs after the first return stroke produced measured field rates-of-change nearly as high as the return stroke rate-of-change, a feature of concern to the protection of aircraft. Many data are available and further study should be performed to expand the sample on which the statistics are based. Pertinent information can be readily extracted by analysis of the DTR records.

We have illustrated the types of data recorded on the WC-130 from all the significant categories observed and derived preliminary characteristics. A large variety appears in the fields recorded on a long time scale (electric field) as well as in the fields recorded on a microsecond scale.

REFERENCES

1. J. C. Corbin, "USAF Lightning-Related Aircraft Accident Statistics," Journal of Defense Research (to be published).

2. J. C. Corbin, "Lightning Interaction with USAF Aircraft," Proceedings of the International Aerospace and Ground Conference on Lightning and Static Electricity, Ft. Worth, Texas, June 1983.

3. J. A. Plumer, "Lightning Effects on General Aviation Aircraft," FAA Conference, Report No. FAA-RD-76-6 Supp 1, Melbourne, FL, March 1979.

4. P. L. Rustan et al., Airborne Lightning Characterization, Flight Dynamics Laboratory, Wright-Patterson Air Force Base, Ohio 45433, AFWAL-TR-83-3013, January 1983.

5. C. E. Baum et al., "Sensors for Electromagnetic Pulse Measurements Both Inside and Away from Nuclear Source Regions," IEEE Transactions on Antennas and Propagation, Vol AP-26, No. 1, January 1978.

6. M. A. Uman et al., "Airborne and Ground-Based Lightning Electric and Magnetic Fields and VHF Source Locations for a Two-Stroke Ground Flash," Proceedings of the International Aerospace and Ground Conference on Lightning and Static Electricity, Ft. Worth, Texas, June 1983.

7. M. A. Uman, "Lightning Data Analysis," Flight Dynamics Laboratory, Wright-Patterson Air Force Base, Ohio 45433, AFWAL-TR-83-3116, December 1983.

8. M. A. Uman and E. P. Krider, "Atmospheric Electricity Hazards Analytical Model Development and Application," Wright-Patterson Air Force Base, Ohio 45433, AFWAL-TR-81-3084, Vol. I, August 1981.

9. M. V. Piepgrass, E. P. Krider and C. B. Moore, "Lightning and Surface Rainfall During Florida Thunderstorms," Journal of Geophysical Research, 87, December 1982.

10. J. M. Livingston and E. P. Krider, "Electric Fields Produced by Florida Thunderstorms," Journal of Geophysical Research, 83, January 1978.

11. P. L. Rustan et al., "Airborne Measurements of the Risetimes in Lightning Return Stroke Fields," Proceedings of the Eighth International Aerospace and Ground Conference on Lightning and Static Electricity, Ft. Worth, Texas, June 1983.

12. C. D. Weidman and E. P. Krider, "The Fine Structure of Lightning Return Stroke Waveforms," Journal of Geophysical Research, 83, December 1978.

REFERENCES (Continued)

13. M. A. Uman et al., "Electric Field Intensity of the Lightning Return Stroke," Journal of Geophysical Research, 78, June 1973.

14. M. A. Uman et al., "Correlated Electric and Magnetic Fields from Lightning Return Strokes," Journal of Geophysical Research, 80, January 1975.

15. Y. T. Lin et al., "Characterization of Lightning Return Stroke Electric and Magnetic Fields from Simultaneous Two-Station Measurements," Journal of Geophysical Research, 84, October 1979.

16. C. D. Weidman and E. P. Krider, "Submicrosecond Risetimes in Lightning Radiation Fields," Geophysical Research Letter, 7, 1980.

17. C. E. Baum et al., "Measurements of Electromagnetic Properties of Lightning with 10 Nanosecond Resolution," Proceedings of the NASA Symposium on Lightning Technology, NASA CP2128, April 1980.

18. D. M. Levine and E. P. Krider, "The Temporal Structure of HF and VHF Radiation During Florida Lightning Return Strokes," Geophysical Research Letter, 4, 1977.

19. W. Beasley, M. A. Uman and P. L. Rustan, "Electric Fields Preceding Cloud-to-Ground Lightning Flashes," Journal of Geophysical Research, 87, June 1982.

20. E. P. Krider, C. D. Weidman and R. C. Noggle, "The Electric Fields Produced by Lightning Stepped Leaders," 82, February 1977.

21. C. D. Weidman and E. P. Krider, "The Radiation Field Waveforms Produced by Intracloud Lightning Discharge Processes," Journal of Geophysical Research, 84, June 1979.

22. E. P. Krider, G. J. Radda and R. C. Noggle, "Regular Radiation Field Pulses Produced by Intracloud Lightning Discharges," Journal of Geophysical Research, 80, September 1975.

23. M. A. Uman, D. K. McLain and E. P. Krider, "The Electromagnetic Radiation from a Finite Antenna," American Journal of Physics, Vol 43, 1975.

24. R. J. Fisher and M. A. Uman, "Measured Electric Field Risetimes for First and Subsequent Lightning Retrun Strokes," Journal of Geophysical Research, 77, January 1972.

25. M. A. Uman et al., "Effects of 200 km Propagation on Florida Lightning Return Stroke Electric Fields," Radio Science, 11, 1976.

REFERENCES (Concluded)

26. B. P. Kuhlman et al., "Lightning Field Spectra Obtained from Airborne Measurements," Proceedings of the International Aerospace and Ground Conference on Lightning and Static Electricity, Ft. Worth, Texas, June 1983.

27. W. P. Geren, "Calibration of C-130 Lightning Characterization Sensors," Flight Dynamics Laboratory, Wright-Patterson Air Force Base, Ohio 45433, AFWAL-TR-82-3095, December 1982.

28. R. K. Baum, "Airborne Lightning Characterization," Proceedings of the NASA Symposium on Lightning Technology, NASA CP2128, April 1980.

29. E. P. Krider and C. D. Weidman, "The Submicrosecond Structure of Lightning Radiation Fields," Proceedings of the International Aerospace and Ground Conference on Lightning and Static Electricity, Ft. Worth, Texas, June 1983.

30. B. G. Melander, "Atmospheric Electricity Threat Definition for Aircraft Lightning Protection," Proceedings of the International Aerospace and Ground Conference on Lightning and Static Electricity, Ft. Worth, Texas, June 1983.

END

FILMED

3-85

DTIC